ul

F L O W   N O I S E

by

Lindsay Hammond Hall

A thesis submitted to the University of London
for the Degree of Doctor of Philosophy in the
Faculty of Science

Department of Mathematics,
Imperial College of Science
and Technology.

February 1969.

Abstract

An exact solution of Lighthill's equation is found when an infinite half plane is introduced into an otherwise unbounded fluid, a finite region of which is turbulent. The two special cases of the turbulent region well within a typical acoustic wavelength of, and many wavelengths from, the edge are discussed in some detail. It is shown that in the first case there is a considerably enhanced acoustic output with the far field intensity depending upon the fifth power of a typical flow Mach number. When the sound producing region is far from the edge it is shown that the resulting sound field has the same features which would be predicted by geometrical acoustics.

The half plane is first supposed to be perfectly rigid but it is then shown that essentially the same results are obtained by allowing the half plane to be a pressure release surface.

In the second part of the thesis an investigation is made into the sound produced by a bubbly flow past an obstacle. The equation of motion of a bubble in such a flow is obtained and it is integrated numerically for the case of an obstacle in the shape of a circular cylinder.

It is found that the bubble's path is considerably different from a fluid streamline. At first the bubble is deflected outwards from the cylinder but later moves within the streamline along which it was originally moving and may appear to strike the cylinder. It is shown that such a bubble suffers a considerable retardation as it nears the cylinder and may disintegrate and so produce appreciable levels of sound. It is shown that bubbles which do not appear to strike the cylinder produce sound levels comparable to those obtained by using the Strasberg hypothesis that the bubble remains on a fluid streamline. It is suggested that sound at the bubble resonance frequency might be excited by means of turbulent fluctuation in the wake and boundary layer associated with the relative motion of the bubble and its surrounding fluid.

It is shown that there is a point upstream of the cylinder on the stagnation streamline where a bubble will come to rest but that bubble oscillations about this point are not possible.

Finally, there is a brief mention of possible changes in the overall sound levels due to changes in the bubble density near the cylinder.

Acknowledgments

The author would like to acknowledge the assistance given him by his supervisor, Dr J. E. Ffowcs Williams, during the course of many friendly discussions over the past three years.

He would also like to acknowledge the generous financial support given him by the Defence Scientific Corps of New Zealand.

Contents

		Page
Abstract		2
Acknowledgments		4
List of Figures		7
Preface		8
Part I		
1.0	Historical Survey and Introduction	11
1.1	The Solution of Lighthill's Equation	15
1.2	The Noise from Eddies very near the Edge	23
1.3	The Noise from Eddies remote from the Edge	32
1.4	The Effect of Motion of the Half Plane	41
1.5	The Effect of Viscosity	44
1.6	General Implications of the Theory	46
1.7	Summary and Conclusions	49
Part II		
2.0	Introduction	51
2.1	The Equation and Motion of a Bubble	54
2.1a	General Considerations	
2.1b	The Equation and Motion of a Bubble in a Flow past a Circular Cylinder	59
2.2	The Bubble Path	63

		Page
2.3	Bubble on the Stagnation Streamline	76
2.4	Acoustic response of a Spherical Bubble to an applied Pressure Field	81
2.5	The Sound produced by a Bubble in a Flow past a Cylinder	85
2.6	Additional sources of sound from a bubbly Flow past an Obstacle	94
Appendix		100

List of Figures

			Page
Figure	1:	The coordinate system	34
"	2:	Sketch of Function IR	34
"	3:		37
"	4:	Bubble Paths	69
"	5:	Bubble Paths	70
"	6:	Bubble Paths for Various R/a	71
"	7:	Bubble Paths if fluid inviscid	72
"	8:	$\frac{d^2 P_a}{dt^2}$ vs. t	87
"	9:	The Fourier Transform of $\frac{d^2 P_a}{dt^2}$	89
"	10:	$\frac{d^2 P_a}{dt^2}$ vs t for bubbles at various from stagnation streamline	92

Preface

This thesis consists of a theoretical investigation into two distinct aspects of a flow past a body.

In the first part a small beginning is made to the answer of the question of what effect a surface containing an edge and immersed in a turbulent fluid has on the sound radiated to large distances. This is done by examining in some detail the sound produced by an infinite half plane, a surface chosen not only because it is the composite of a very simple edge (plane and linear) and a surface whose acoustic effects on a turbulent fluid are well understood, but more prosaically, because it has the simplest Green's function appropriate to Helmholtz's equation of all surfaces which have edges.

At the end of the necessarily rather tedious mathematical analysis the applicability and relevance of the conclusions drawn from this highly idealised surface to surfaces of dimensions encountered in the real world must, unhappily, remain an open question. Optimistically, we might hope that the sound from surfaces such as hydroplanes or marine propellor blades might have features in common with that of the infinite half plane.

The sound from near a marine propellor is the subject of the second part of this thesis but now it is not the turbulence of the surrounding water which is the ultimate origin of the sound but rather the presence in this water of air bubbles. For a surface vessel these bubbles may have arisen from an upstream cavitating region or simply from the entrainment of the bow wave tumbling ahead of the ship. In a modern submarine bubbles are often released in an effort to reduce the overall radiated sound levels. In any event the situation where we have a bubbly flow past an obstacle (such as a propellor blade) frequently occurs in underwater situations and so there is some interest in assessing the possible acoustic consequences. Again a grossly oversimplified model must be adopted and here we replace our finite body from the real world with an infinite circular cylinder and perform our hypothetical experiments in that yet undiscovered part of the globe where gravity does not act.

PART I

1.0 Historical Background and Introduction

Modern theories on the production and estimation of the noise radiated by a turbulent fluid date from Lighthill's two papers[1,2] "On Sound Generated Aerodynamically". The effect of material surfaces within the fluid was not considered beyond a brief footnote in the second paper which indicated that the forces acting at such surfaces could produce dipole sound fields. This deficiency was made good by Curle[3] in 1955 who used the Kirchoff solution of the inhomogeneous wave eauation to show that when boundaries are present the volume quadrupole sources are augmented by surface distributions of dipoles and monopoles, the dipole strength density being eaual to the stress exerted on the fluid by the boundary. Given the greater radiative efficiency of dipole sources compared to quadrupoles in low Mach number flows, Curle was able to explain the observed directionality of Aeolian sound. However, it soon became apparent that care was needed in the application of Curle's result to surfaces whose dimensions were not much less than a typical acoustic wavelength - that is, to surfaces no longer "acoustically compact". Fint Phillips[4], in an argument later criticised by Lighthill[5], showed that the dipole strengths should vanish for a plane turbulent boundary layer flow which was homogeneous in layers parallel to the surface. Then, in 1960, Powell[6] showed that on a plane rigid boundary supporting an inviscid flow, the pressure dipole terms simply account for the reflection in the surface of the quadrupole sources in the basic flow. About the same time as Powell's paper Doak[7] showed how Lighthill's equation could be solved formally by the method of Green's functions, Curle's formula appearing if a certain choice of Green's function is made. By choosing different Green's functions different solutions which emphasise different sources can be obtained - solutions which though differing in form are nevertheless equivalent. Doak concluded that dipole radiation is predominant for low Mach number flows from a flat plate but that perfectly rigid or perfectly soft surfaces of arbitrary shape produce only quadrupole sound. None of these conclusions still stands. In 1964 Ffowcs Williams[8] developed Powell's idea of using a null solution of the wave equation to show that an infinite plane unsupported homogeneous surface of arbitrary surface impedance supporting a turbulent boundary layer produces radiation entirely of a quadrupole nature, simple surface supports later[9] being shown to produce dipole sound. In 1966 Leppington[10] showed that the diffracted field of a longitudinal quadrupole oriented radially towards a rigid sphere has a farfield strength comparable to that of a dipole provided the sphere is well within the nearfield of the quadrupole. Leppington's result has importance for it provides a theoretical - as opposed to experimental - demonstration that Curle's dipole has non-vanishing integrated strength for at least one shape of an acoustically compact body.

Now a distinguishing feature of those surfaces which have, unambiguously, been shown to produce dipole sound and those which produce quadrupole sound is that when a sound wave is incident on the former surfaces a diffracted sound field is produced, but not when the surface is of the second sort. It is possible that the enhanced acoustic output is somehow associated with this diffracted field. Any diffracted field depends of course on the geometry of the diffracting object and in particular on the edges of the body. An investigation into the effect of variously shaped edges would therefore be of considerable interest and it is the purpose of this work to discuss in some detail the simplest of all possible edges, namely, that of a semi-infinite plane.

The procedure which is followed is to obtain a solution of the Fourier transform of Lighthill's equation by means of a Green's function obtained by Macdonald[11] which is exact for points in the farfield. The half plane is supposed to be vanishingly thin but perfectly rigid. This is done in Section 1.1. In Section 1.2 the case of an eddy very near the edge is discussed and it is shown using a dimensional analysis that the acoustic output from such an eddy depends upon the fifth power of some typical flow velocity. In Section 1.3 the turbulent region is supposed to be far from the edge and it is found that the sound field is that which would have been predicted by geometrical acoustics. In the next section (1.4) the condition that the half plane be rigid is changed so that the half plane is taken to be a perfect pressure release surface. Sensibly the same results are obtained as for the rigid case. In Section 1.5 the effect of viscosity is briefly discussed and it is concluded that any effect is negligible. Finally, in Section 1.6, some implications are drawn from the preceding theory. In particular it is shown that for any surface likely to be encountered in underwater applications the noise from an edge region will always be dominant.

1.1 The Solution of Lighthill's Equation

The basic equation which describes aerodynamic noise generation and propagation and which is taken as the starting point of this analysis is due to Lighthill (1952)

$$\nabla^2 \rho - \frac{1}{c^2}\frac{\partial^2 \rho}{\partial t^2} = -\frac{1}{c^2}\frac{\partial^2}{\partial y_i \partial y_j}\left(\rho v_i v_j + p_{ij} - c^2\rho\delta_{ij}\right) \qquad \text{---} (1)$$

where ρ is the fluid density, (v_1, v_2, v_3) the velocity vector, c the sound speed in the undisturbed fluid and p_{ij} the compressive stress tensor. We shall initially assume that viscous effects are negligible so that we set p_{ij} equal to $p\delta_{ij}$, where p is the isotropic pressure in the fluid. If we further suppose that changes in p are exactly balanced by changes in $c^2\rho$ then Lighthill's equation can be written

$$\nabla^2 p - \frac{1}{c^2}\frac{\partial^2 p}{\partial t^2} = -\frac{\partial^2 \rho v_i v_j}{\partial y_i \partial y_j} \qquad \text{---} (2)$$

We seek a solution of this equation when there is a rigid, vanishingly thin, half-plane immersed in an otherwise unbounded fluid.

If we define the generalised Fourier transform of the function $f(t)$ as

$$f^*(\omega) = \frac{1}{2\pi}\int_{-\infty}^{\infty} f(t)\, e^{-i\omega t}\, dt$$

then Lighthill's equation can be written as the inhomogeneous Helmholtz equation

$$\nabla^2 p^* + k^2 p^* = -\left(\frac{\partial^2 \rho v_i v_j}{\partial y_i \partial y_j}\right)^* \qquad \text{--}(3)$$

where $k = \dfrac{\omega}{c}$

The presence of the rigid half plane gives the boundary condition that the normal velocity vanishes at the surface. The solution of (3) with this boundary condition can be written down at once in terms of a Green's function, G, whose normal derivative vanishes on the half-plane. It is

$$p^*(\underline{x},\omega) = \frac{1}{4\pi}\int\left(\frac{\partial^2 \rho v_i v_j}{\partial y_i \partial y_j}\right)^* G\, dV(\underline{y}) + \frac{1}{4\pi}\int_{\text{half-plane}} \frac{\partial p^*}{\partial n} G\, dS \qquad \text{--}(4)$$

$$\left.\begin{aligned} &\text{where } (\nabla^2 + k^2)\,G = -4\pi\,\delta(\underline{x} - \underline{y}) \\ &\text{with } \frac{\partial G}{\partial n} = 0 \qquad \text{on the half-plane} \end{aligned}\right\} (5)$$

The volume integral in (4) is strictly over all space but as $\left(\frac{\partial^2 \rho v_i v_j}{\partial y_i \partial y_j}\right)^*$ is considered non zero only within the turbulence the volume integral need be evaluated only over that region. If we now complete the divergences in (4), and convert the volume divergence integrals into surface integrals by the use of Gauss' theorem we find that the surface integrals vanish because of the condition that there is no normal velocity on the half-plane and we are left with

$$4\pi p^*(\underline{x}, \omega) = \int (\rho v_i v_j)^* \frac{\partial^2 G}{\partial y_i \partial y_j}\, dV(\underline{y}) \quad \text{--}(6)$$

In cylindrical polars this is

$$4\pi p^*(r, \theta, z; \omega) = \int \Big\{ \rho v_r^2 \frac{\partial^2 G}{\partial r^2} + \rho v_z^2 \frac{\partial^2 G}{\partial z_0^2}$$

$$+ \rho v_r v_z \left(\frac{\partial}{\partial r_0}\left(\frac{\partial G}{\partial z_0}\right) + \frac{\partial}{\partial z_0}\left(\frac{\partial G}{\partial r_0}\right)\right)$$

$$+ \rho v_r v_\theta \left(\frac{\partial}{\partial r_0}\left(\frac{1}{r_0}\frac{\partial G}{\partial \theta_0}\right) + \frac{1}{r_0}\frac{\partial}{\partial \theta_0}\left(\frac{\partial G}{\partial r_0}\right) - \frac{1}{r_0^2}\frac{\partial G}{\partial \theta_0} \right)$$

$$+\rho v_\theta v_z \left(\frac{1}{r_0} \frac{\partial}{\partial \theta_0}\left(\frac{\partial G}{\partial z_0}\right) + \frac{\partial}{\partial z_0}\left(\frac{1}{r_0}\frac{\partial G}{\partial \theta_0}\right)\right.$$

$$\left. + \rho v_\theta^2 \left(\frac{1}{r_0^2} \frac{\partial^2 G}{\partial \theta_0^2} + \frac{1}{r_0}\frac{\partial G}{\partial r_0}\right)\right\}^* dV_0 \qquad ----(8)$$

where $dV_0 = r_0 \, dr_0 \, d\theta_0 \, dz_0$

The particular cylindrical coordinate system which we use is illustrated in figure 1.

We restrict our attention to field points which are many wavelengths both from the turbulent region and from the edge of the half-plane. That is, we suppose

and $kr >> 1$ and $r >> r_0$

Macdonald[12] (1915) has shown that the solution of (5) takes, in the far field, the form:

$$G = \frac{e^{i\pi/4}}{\sqrt{\pi}} \left\{ \frac{e^{-ikR}}{R} \int_{-\infty}^{u_R} e^{-iu^2} du + \frac{e^{-ikR'}}{R'} \int_{-\infty}^{u_{R'}} e^{-iu^2} du \right\} \quad --(9)$$

where

$$u_R = 2\left(\frac{krr_0}{D+R}\right)^{\frac{1}{2}} \cos\frac{\theta-\theta_0}{2} = \pm\left[k(D-R)\right]^{\frac{1}{2}}$$

and

$$u_{R'} = 2\left(\frac{krr_0}{D+R'}\right)^{\frac{1}{2}} \cos\frac{\theta+\theta_0}{2} = \pm\left[k(D-R')\right]^{\frac{1}{2}}$$

R is the separation of the source point (r_0, θ_0, z_0)

and the field point (r, θ, z)

i.e. $R = \left\{ r^2 + r_0^2 - 2 r r_0 \cos(\theta - \theta_0) + (z - z_0)^2 \right\}^{\frac{1}{2}}$

R' is the separation of the specular image source point in the plane containing the half plane, $(r_0, -\theta_0, z_0)$, and the field point.

$$R' = \left\{ r^2 + r_0^2 - 2 r r_0 \cos(\theta + \theta_0) + (z - z_0)^2 \right\}^{\frac{1}{2}}$$

$$D = \left\{ (r + r_0)^2 + (z - z_0)^2 \right\}^{\frac{1}{2}}$$

It can be shown that D is the shortest distance between the source and field points travelling via the edge.

G is similar to the Green's function for an infinite rigid plane with the difference that now each term is weighted by a Freshel integral whose magnitude can vary between 0 and 1 (approximately). Any enhancement of the sound field from that produced by turbulence in free space or near a rigid plane can only arise from the derivatives of these integrals, and in particular, from the derivatives of U_R and $U_{R'}$.

The limits of integration u_R and $u_{R'}$ may be simplified by noting that any derivative of the factors $(D + R)^{-\frac{1}{2}}$ or $(D + R')^{-\frac{1}{2}}$ does not appear in the farfield representation of p^* when G is substituted into (8) . We may therefore use at once the farfield approximations

$$D + R \approx 2\left\{ r^2 + (z - z_0)^2 \right\}^{\frac{1}{2}}$$

and $$D + R' \approx 2\left\{ r^2 + (z - z_0^2) \right\}^{\frac{1}{2}}$$

to write

$$u_R = (2 k r_0 \sin\phi)^{\frac{1}{2}} \cos\frac{\theta - \theta_0}{2}$$

and $$u_{R'} = (2 k r_0 \sin\phi)^{\frac{1}{2}} \cos\frac{\theta + \theta_0}{2}$$

where $$\sin\phi = \frac{r}{\sqrt{r^2 + (z - z_0)^2}}$$

The independence in the farfield of u_R and $u_{R'}$ on the coordinate z_0 excludes the possibility that the term $\int (\rho v_2^2)^* \frac{\partial^2 Y}{\partial z_0^2}\, dV_0$ in (8) might have a magnitude much greater than if G were just that of a rigid plane.

Accordingly, we can conclude immediately that the edge does not result in any significant enhancement of the sound produced by longitudinal quadrupoles aligned parallel with the edge.

Also, another deduction can be made from the general form of G, namely, that the sound field at points on the plane $\theta = \pi$ has exactly the same features as sound from free turbulence. This may be seen as follows. On the plane $\theta = \pi$ (which is the half plane complementary to the material half plane) the field point is equidistant from the real and image source points. That is, R = R' and so

$$G = \frac{e^{i\pi/4}}{\sqrt{\pi}} \frac{e^{-ikR}}{R} \left\{ \int_{-\infty}^{2\left(\frac{krr_0}{D+R}\right)^{\frac{1}{2}} \sin\frac{\theta_0}{2}} e^{-iu^2}\, du + \int_{-\infty}^{-2\left(\frac{krr_0}{D+R}\right)^{\frac{1}{2}} \sin\frac{\theta_0}{2}} e^{-iu^2}\, du \right\}$$

$$= \frac{e^{i\pi/4}}{\sqrt{\pi}} \frac{e^{-ikR}}{R} \left\{ 2\int_{0}^{\infty} e^{-iu^2}\, du + \int_{\infty}^{2\left(\frac{krr_0}{D+R}\right)^{\frac{1}{2}} \sin\theta_0/2} e^{-iu^2}\, du + \int_{0}^{-2\left(\frac{krr_0}{D+R}\right)^{\frac{1}{2}} \sin\theta_0/2} e^{-iu^2}\, du \right\}$$

$= \dfrac{e^{-ikR}}{R}$, the Green's function for an unbounded fluid.

We are now ready to substitute the expression for G given by (9) into the equation for $p^*(r, \theta, z; \omega)$. We shall consider separately the two cases of turbulence well within a typical acoustic wavelength of the edge and many wavelengths away from the edge.

1.2 The Noise from Eddies very near the Edge

We first consider the case of eddies (that is, regions of the turbulence over which fluctuations of velocity are highly correlated) which are well within a wavelength of the edge. By this we mean that every part of the eddy satisfies the inequality

$$2kr_0 << 1 .$$

The Freshel integral $\dfrac{e^{-i\pi/4}}{\sqrt{\pi}} \displaystyle\int_{-\infty}^{X} e^{-iu^2} du$

has the series expansion

$$\frac{e^{i\pi/4}}{\sqrt{\pi}} \int_{-\infty}^{X} e^{-iu^2} du = \frac{1}{2} + \frac{e^{i\pi/4}}{\sqrt{\pi}} X \left(1 - \frac{i}{3} X^2 + O(X^4)\right).$$

(see, for example, the introduction to Pearcey's (1956) Tables[13]).

Hence we can write

$$\mathcal{G} = \frac{e^{-ikR}}{R}\left(\frac{1}{2} + \frac{e^{i\pi/4}}{\sqrt{\pi}}(2kr\sin\phi)^{\frac{1}{2}}\cos\frac{\theta-\theta_0}{2}\left(1+O(kr_0)\right)\right)$$

$$+ \frac{e^{-ikR'}}{R'}\left(\frac{1}{2} + \frac{e^{i\pi/4}}{\sqrt{\pi}}(2kr_0\sin\phi)^{\frac{1}{2}}\cos\frac{\theta+\theta_0}{2}\left(1+O(k_0)\right)\right)$$

Or, noting that

$$kR' = kR + 2kr_0\sin\theta_0\sin\theta + O\left(\frac{kr_0^2}{R}\right)$$

we can replace R' by R

$$G = \frac{e^{-ikR}}{R}\left(1 + \frac{2e^{i\pi/4}}{\sqrt{\pi}}(2kr_0 \sin\phi)^{\frac{1}{2}} \times \right.$$
$$\left. \cos\frac{\theta_0}{2}\cos\theta/2 + O(kr_0)^{3/2} \right) \quad ----(10)$$

When this expression for G is fed with equation 8 we obtain terms containing $(2kr_0)^{-3/2}$, $(2kr_0)^{-\frac{1}{2}}$ or positive powers of $2kr_0$. Under the condition $2kr_0 \ll 1$ the dominant terms are those containing $(2kr_0)^{-3/2}$ and it is these terms we retain when we write

$$4\pi p^*(r, \theta, z ; w) = k^2 \frac{2e^{i\pi/4}}{\sqrt{\pi}}(\sin\phi)^{\frac{1}{2}}\cos\theta/2 \times$$
$$\int\left\{\rho v_r^2\cos\theta_0/2 - \rho v_\theta^2\cos\theta_0/2 + 2\rho v_r v_\theta \sin\theta_0/2\right\}^* \times$$
$$(2kr_0)^{-3/2}\frac{e^{-ikR}}{R}\,dV_0 \quad ----(11)$$

where the volume integral is evaluated over those eddies which satisfy $2kr_0 << 1$

This equation is the basic result of this section. It is exactly the same result as is obtained by performing the differentiations on the Green's function in the form (9) and then picking out the dominant terms under the condition $2kr_0 << 1$. It should be compared with the corresponding equation which is applicable to an unbounded turbulent fluid:

$$4\pi p^*(r, \theta, z; \omega) = -k^2 \int \Big\{ \rho v_r^2 \cos^2(\theta - \theta_0) + \rho v_\theta^2 \sin^2(\theta - \theta_0) + 2\rho v_r v_\theta \cos(\theta - \theta_0)\sin(\theta - \theta_0)$$

+ similar terms involving <u>each</u> of the remaining Reynold stresses $\Big\}^* \dfrac{e^{-ikR}}{R} \, dV_0$ ----(12)

The first point to notice is that the integrand of (11) contains the large factor $(2kr_0)^{-3/2}$. This has the consequence that the farfield acoustic pressure levels when there is an edge in the turbulent region may be considerably greater than when there is none. "May be", because the pressure field has a different directionality to that of the radiation field of an eddy in free turbulence. This feature is not entirely novel. Leppington has shown that the diffracted farfield component of a point harmonic source near a rigid sphere has the form

$$\frac{e^{-ikr}}{r} \frac{h_1(kr_0)}{h_1'(ka)} \cos\psi_0$$

where $\cos\psi_0 = \cos\theta\cos\theta_0 + \sin\theta\sin\theta_0\cos(\phi - \phi_0)$

(r, θ, ϕ) and (r_0, θ_0, ϕ_0) are spherical polar co-ordinates of the field point and source point respectively, relative to an origin at the centre of the sphere, which has radius a.

$h_1(z)$ is a spherical Bessel function of the third kind.

$h_1'(z)$ means $\frac{d}{dz}(h_1(z))$

If kr_0, $ka << 1$ then

$$\frac{h_1}{h_1'} \sim -\frac{ka^3}{2r_0^2}$$

If this is now used as part of the Green's function for the formal solution of equation (3) in the presence of a rigid sphere, one of the terms obtained under the condition $kr_0 << 1$ (arising from

$$\int (\rho v_r^2)^* \frac{\partial^2 G}{\partial r_0^2} dV_0 \quad)$$

is

$$\int 3\frac{e^{-ikr}}{r} \cos\psi_0\, k^2 (ka)\frac{a^2}{r_0^2}\left(\frac{1}{kr_0}\right)^2 (\rho v_r^2)^* dV_0$$

corresponding to an enhancement by the factor

$3(ka)\frac{a^2}{r_0^2}\left(\frac{1}{kr_0}\right)^2$ on the free turbulence value.

A further point to notice is that the different Reynolds stresses are differently affected by the half-plane. The stresses $\rho v_r^2, \rho v_\theta^2$ and $\rho v_r v_\theta$ produce pressure fields which are greater by a factor of order $(2kr_0)^{-3/2}$ on the free turbulence values; the stresses $\rho v_r v_z$ and $\rho v_\theta v_z$ (which are not shown in (11)) are increased by the smaller factor $(2kr_0)^{-\frac{1}{2}}$, while the stress ρv_z^2 has just the pressure field we would expect if the half-plane was an infinite plane (i.e., had no edge).

Following Lighthill, we regard the turbulence as divided into regions within which each of the products $(\rho v_r^2)^*$, $(\rho v_\theta^2)^*$ and $(\rho v_r v_\theta)^*$ is perfectly correlated, the size of each region being very much less than an acoustic wavelength. For the sound pressure from such a region we can write

$$4\pi p^*(r,\theta,z;\omega) = k^2\frac{2e^{i\pi/4}}{\sqrt{\pi}}(\sin\phi)^{\frac{1}{2}}\cos\theta/_2\ \frac{e^{-ikR}}{R}$$

$$\times \left[(\rho v_r^2 - \rho v_\theta^2)^* \int \cos \theta_0/_2 \, (2kr_0)^{-3/2} dV_0 \right.$$

$$\left. + 2(\rho v_r v_\theta)^* \int \sin \theta_0/_2 \, (2kr_0)^{-3/2} dV_0 \right]$$

$$\text{.....} \quad (13)$$

where the volume integrals are now to be evaluated over the region of perfect correlation. If such a region is supposed to occupy the space $r_1 < r_0 < r_2$, $\theta_1 < \theta_0 < \theta_2$ and $z_1 < z_0 < z_2$ then a good approximation to these volume integrals is $2^{\frac{1}{2}} \begin{smallmatrix}\cos\\ \sin\end{smallmatrix} \beta/_2 \, (k\bar{r}_0)^{-3/2} V$ where the cos or sin is to be taken if the original integral contained a cos or a sin, V is the volume of the eddy and $\beta = \dfrac{\theta_1 + \theta_2}{2}$ and $\bar{r}_0 = \dfrac{r_1 + r_2}{2}$. $\bar{r}_0, \beta$ may be regarded as the r_0, θ_0 coordinates of the centre of the eddy. It is assumed that $\sin \dfrac{\theta_2 - \theta_1}{2} \doteqdot \dfrac{\theta_2 - \theta_1}{2}$.

The volume integrals may also be evaluated if it is supposed that the eddy is a cylinder centred on the edge of the half-plane. The integrals containing $\cos \theta_0/_2$ vanish but

$$\int \sin\theta/_2\,(2kr_o)^{-3/2}\,dV_o = \frac{2^{7/2}}{\pi}\,(k\delta)^{-3/2}\,V$$

$$= 2^{\frac{1}{2}}\,(1{\cdot}3\,k\delta)^{-3/2}\,V\,,$$

where 2 is the diameter of the cylinder. This result indicates that a lower bound for $\bar{r}_s$ should be 1.3 , or, roughly, δ .

If we write $v_r = U_r + u_r$, $v_\theta = U_\theta + u_\theta$ and $v_z = U_z + u_z$ where the flow near the edge is regarded as being composed of a steady, time independent part (U_r, U_θ, U_z) and a fluctuating part (u_r, u_θ, u_z) then, for example,

$$(\rho v_r^2)^* = \rho_o\,(U_r^2 + 2U_r u_r + u_r^2)^*$$

$$= 2\rho_o\,U_r u_r^*$$

where ρ has been set equal to ρ_o , the density of the undisturbed fluid. U_r^2, because it is independent of time, makes no contribution and the term u_r^2 is neglected because it is smaller than the term $U_r u_r$ by the factor of α, the turbulence intensity. That is u_r is of order α times a typical flow velocity (U say)

Instead of (13) we may now write the approximate relation

$$4\pi p^* = 4\left(\frac{2}{\pi}\right)^{\frac{1}{2}} k^2 \cos\theta/2 \,(\sin\phi)^{\frac{1}{2}} \frac{e^{-ikR}}{R} \rho_0 U^2 \alpha \sin\bar{\theta} \times \frac{\cos}{\sin} \theta/2 \,(k\bar{r}_0)^{-3/2} \, \bar{V} \quad \text{--- (14)}$$

where $\bar{\theta}$ is the angle the mean flow makes with the edge of the half-plane. From this we can obtain an approximate formula for the farfield acoustic intensity that neglects any effects of cross correlation between individual terms of (13). It is

$$I(r,\theta,z;\omega) \doteq \frac{k^4 \sin\phi \cos^2\frac{\theta}{2} \rho_0 U^4 \alpha^2 \sin^2\bar{\theta} \frac{\cos^2}{\sin^2}\theta/2 \, \bar{V}^2}{\pi^3 c \, R^2 \,(k\bar{r}_0)^3} \quad \text{--- (15)}$$

Setting $\bar{r}_0$ equal to the correlation radius we find I has a maximum value of

$$I_{max} \doteq \frac{\rho k^4 U^4 V^2}{\pi^3 c R^2 \delta^3} \quad \text{---- (16)}$$

The typical frequency of the turbulent source is of order $\frac{U}{2\delta}$ so that k is of order $\frac{\pi U}{c\delta}$. <u>Thus the scattered intensity increases in proportion to the</u>

<u>fifth power of the fluid velocity, U</u>. This is a new result which should be compared to the eighth power low obtained from free turbulence or turbulence supported by an infinite plane and the sixth power law obtained from the usual estimations of Curle's (1956) surface dipole term. Curle's solution of Lighthill's equation in the presence of surfaces has been examined by numerous workers and is undoubtedly correct. However, the difficulty with his result is that it is not possible to estimate quantitatively the consequences of the "dipole" term for surfaces which are not small compared with an acoustic wavelength. Dimensional arguments are altogether too crude: for infinite planes they overestimate the sound and for semi-infinite planes they under estimate it.

1.3 The Noise from Eddies remote from the Edge

We now consider the effect of the half-plane on the noise from those eddies which are far enough from the edge for the inequality $(k\bar{r}_o)^{\frac{1}{2}} >> 1$ to hold. $\bar{r}_o$ is again the distance of the centre of the eddy from the edge.

We write G in Macdonald's form:

$$\left.\begin{aligned} G &= \frac{e^{-ikR}}{R} I_R + \frac{e^{-ikR'}}{R'} I_{R'} \\ \text{where} \quad I_R &= \frac{e^{i\pi/4}}{\sqrt{\pi}} \int_{-\infty}^{u_R} e^{-iu^2} du \\ \text{and} \quad I_{R'} &= \frac{e^{i\pi/4}}{\sqrt{\pi}} \int_{-\infty}^{u_{R'}} e^{-iu^2} du \end{aligned}\right\} \quad (17)$$

When G is substituted into equation (8) for p^* and the factor k^2 abstracted from each term, three distinct sets of terms are obtained; those containing the factor I_R or $I_{R'}$, those containin g the factor $(kr_o)^{-\frac{1}{2}}$ and, finally, those with the factor $(kr_o)^{-3/2}$

For example,

$$\int (\rho v_\theta^2)^* \left\{ \frac{1}{r_o^2} \frac{\partial^2}{\partial \theta_o^2} + \frac{1}{r_o} \frac{\partial}{\partial r_o} \right\} \frac{e^{-ikR}}{R} I_R \, dV_o$$

$$= \int (\rho v_\theta^2)^* \left\{ \frac{1}{r_o} \frac{\partial}{\partial \theta_o} \left(e^{-ikR} \frac{1}{r_o} \frac{\partial I_R}{\partial \theta_o} \right) \right.$$

$$-ik\left(\frac{1}{r_o^2}\frac{\partial^2 R}{\partial\theta_o^2}+\frac{1}{r_o}\frac{\partial R}{\partial\theta_o}\right)e^{-ikR}$$

$$-ik\ \frac{1}{r_o}\frac{\partial R}{\partial\theta_o}\ \frac{1}{r_o}\frac{\partial I_R}{\partial\theta_o}\ e^{-ikR}$$

$$-k^2\left(\frac{1}{r_o}\frac{\partial R}{\partial\theta_o}\right)^2 e^{-ikR}\, I_R$$

$$+\frac{1}{r_o}\, e^{-ikR}\ \frac{\partial I_R}{\partial r_o}\ \Bigg\}\ \frac{dV_o}{R} \qquad \text{--- (18)}$$

Derivatives of $\frac{1}{R}$ have been omitted because they do not appear in the farfield. Neither does the term containing

$$\frac{1}{r_o^2}\frac{\partial^2 R}{\partial\theta_o^2}+\frac{1}{r_o}\frac{\partial R}{\partial\theta_o}$$

Now

$$e^{-ikR}\frac{1}{r_o}\frac{\partial I_R}{\partial\theta_o}=e^{-ikR}\frac{e^{i\pi/4}}{\sqrt{\pi}}e^{-iu_R^2}\frac{1}{r_o}\frac{\partial u_R}{\partial\theta_o}$$

$$=k\frac{e^{i\pi/4}}{\sqrt{\pi 2}}e^{-ikD}(kr_o)^{-\frac{1}{2}}\sin\frac{\theta-\theta_o}{2}(\sin\phi)^{\frac{1}{2}}$$

so that $$\frac{1}{r_o}\frac{\partial}{\partial\theta_o}\left(e^{-ikR}\frac{1}{r_o}\frac{\partial I_R}{\partial\theta_o}\right)=-\frac{1}{2}k^2\frac{e^{i\pi/4}}{\sqrt{2\pi}}e^{-ikD}(kr_o)^{-3/2}\cos\frac{\theta-\theta_o}{2}(\sin\phi)^{\frac{1}{2}}$$

Also

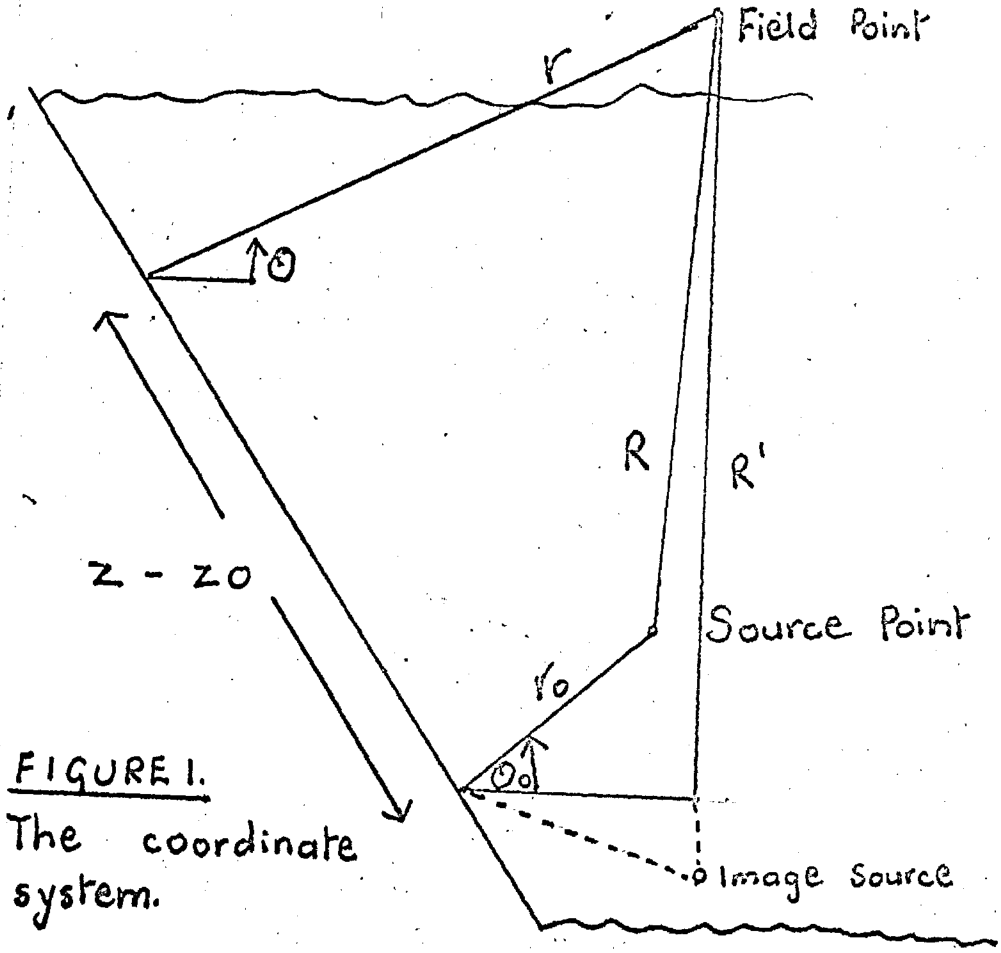

FIGURE 1.
The coordinate system.

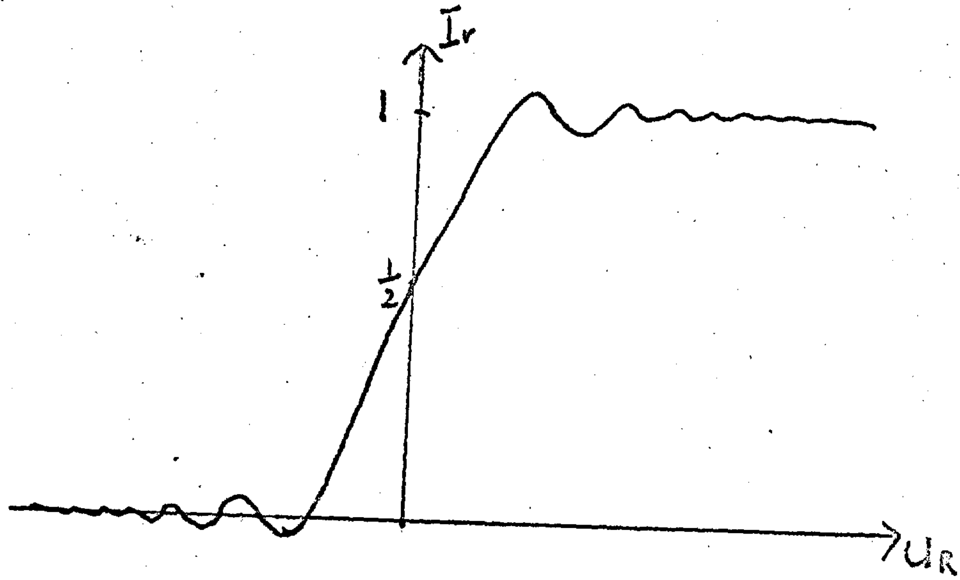

FIGURE 2.
Sketch of the function I_R.

$$e^{-ikR}\frac{1}{r_0}\frac{\partial I_R}{\partial r_0} = k^2\frac{e^{i\pi/4}}{\sqrt{2\pi}}e^{-ikD}(kr_0)^{-3/2}\cos\frac{\theta-\theta_0}{2}(\sin\phi)^{\frac{1}{2}}$$

Combining these results, we have instead of

$$\int(\rho v_\theta^2)^*\left\{\frac{1}{r_0^2}\frac{\partial^2}{\partial\theta_0^2}+\frac{1}{r_0}\frac{\partial}{\partial r_0}\right\}\frac{e^{-ikR}}{R}I_R\,dV_0$$

$$= -k^2\int(\rho v_\theta^2)^*\left\{\left(\frac{1}{r_0}\frac{\partial R}{\partial\theta_0}\right)^2 e^{-ikR}I_R\right.$$

$$-i\frac{1}{r_0}\frac{\partial R}{\partial\theta_0}\frac{e^{i\pi/4}}{\sqrt{2\pi}}e^{-ikD}(kr_0)^{-\frac{1}{2}}\sin\frac{\theta-\theta_0}{2}(\sin\phi)^{\frac{1}{2}}$$

$$\left.+\frac{1}{2}\frac{e^{i\pi/4}}{\sqrt{2\pi}}e^{-ikD}(kr_0)^{-3/2}\cos\frac{\theta-\theta_0}{2}(\sin\phi)^{\frac{1}{2}}\right\}\frac{dV_0}{R} \quad -(19)$$

The remaining terms on the right hand side of equation (8) can be dealt with similarly.

Figure 2 shows a sketch of the behaviour of I_R $(I_{R'})$ as a function of u_R $(u_{R'})$. It is apparent that if $(kr_0)^{\frac{1}{2}}$ is very large and u_R $(u_{R'})$ is not large and negative then the terms containing I_R $(I_{R'})$ are much larger than those containing $(kr_0)^{-\frac{1}{2}}$ and $(kr_0)^{-3/2}$. The signs of u_R and $u_{R'}$ depend upon the signs of $\cos\frac{\theta-\theta_0}{2}$ and $\cos\frac{\theta+\theta_0}{2}$ respectively. If both $\cos\frac{\theta-\theta_0}{2}$ and $\cos\frac{\theta+\theta_0}{2}$ are positive - and this will be the case if θ is acute and $\theta_0 \doteq \pi - \theta$ then

$$4\pi p^* = -k^2 \int (\rho v_i v_j)^* \left[R_i R_j \frac{e^{-ikR}}{R} I_R + R_i' R_j' \frac{e^{-ikR'}}{R'} I_{R'} \right] dV_0 \qquad \text{--- (20)}$$

where

$$(v_i) = (v_r, v_\theta, v_z)$$

$$(R_i) = \left(\frac{\partial R}{\partial r_0}, \frac{1}{r_0}\frac{\partial R}{\partial \theta_0}, \frac{\partial R}{\partial z_0} \right)$$

and

$$(R_i') = \left(\frac{\partial R'}{\partial r_0}, \frac{1}{r_0}\frac{\partial R'}{\partial \theta_0}, \frac{\partial R'}{\partial z_0} \right)$$

If θ_0 is just a little greater than $\pi - \theta$ so that $u_{R'}$, although negative, still has $I_{R'}$ with magnitude much greater than $(kr_0)^{-\frac{1}{2}}$ then (20) is still the appropriate expression for p^*. For larger values of θ_0, but θ_0 still less than $\pi + \theta$, $I_{R'}$ has magnitude comparable to $(kr_0)^{-\frac{1}{2}}$ and so is negligible compared to I_R which is, at least, greater than $\frac{1}{2}$. When θ_0 is in this range the expression for p^* is

$$4\pi p^*(r, \theta, z; \omega) = -k^2 \int (\rho v_i v_j)^* R_i R_j \frac{e^{-ikR}}{R} I_R \, dV_0 \qquad \text{--- (21)}$$

Again, if θ_0 is a little greater than $\pi + \theta_0$, I_R is still much greater than $(kr_0)^{-\frac{1}{2}}$ and (21) is still

FIGURE 3

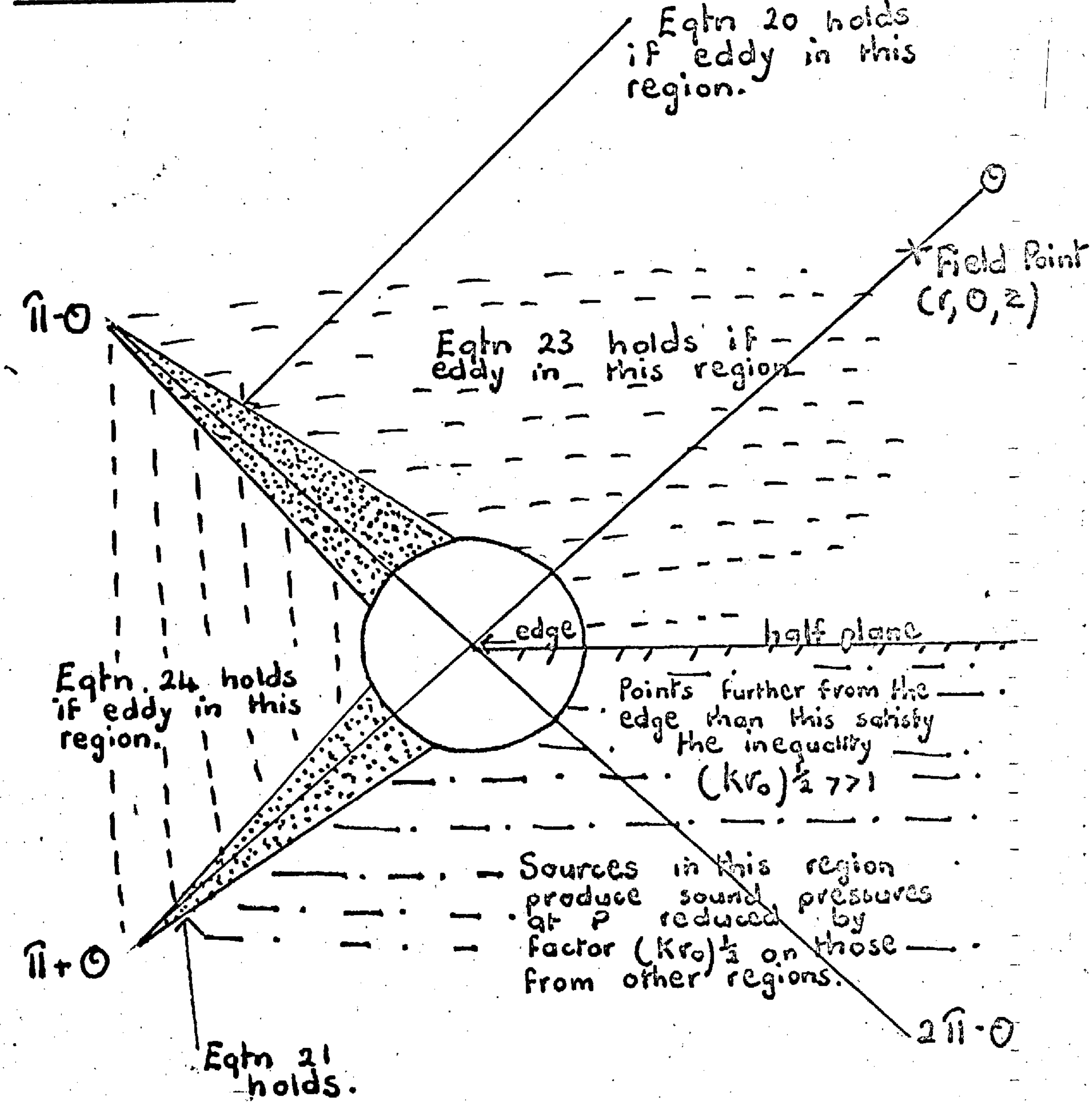
Eqtn 20 holds if eddy in this region.
Field Point (r, θ, z)
θ
π-θ
Eqtn 23 holds if eddy in this region
edge
half plane
Eqtn. 24 holds if eddy in this region.
Points further from the edge than this satisfy the inequality (kr₀)^½ >> 1
Sources in this region produce sound pressures at P reduced by factor (kr₀)^½ on those from other regions.
π+θ
2π-θ
Eqtn 21 holds.

applicable. For larger θ_0, however, both I_R and $I_{R'}$ are comparable to $(kr_0)^{-\frac{1}{2}}$. The expression for p^* would now have to include not only the terms containing I_R and $I_{R'}$ but also those containing the factor $(kr_0)^{-\frac{1}{2}}$. We shall not write this expression down but merely note that the value of p^* which it would predict is much smaller, by the factor $(kr_0)^{-\frac{1}{2}}$, from the values given by (20) or (21).

Now (see Pearcey)

$$\frac{e^{i\pi/4}}{\sqrt{\pi}}\int_{-\infty}^{X} e^{-iu^2}\,du \sim 1 + \frac{e^{i\pi/4}}{2\sqrt{\pi}}\frac{e^{-iX^2}}{X} \quad \text{as } X \to \infty \qquad (22)$$

so that, except near $\theta_0 = \pi - \theta$, we can write (20) as

$$4\pi p^*(r,\theta,z;\omega) = -k^2\int (\rho v_i v_j)^*\left[R_i R_j \frac{e^{-ikR}}{R} + R_i' R_j' \frac{e^{-ikR'}}{R'}\right] dV_0 \qquad -(23)$$

and equation (21) as

$$4\pi p^*(r,\theta,z,\omega) = -k^2\int (\rho v_i v_j)^* R_i R_j \frac{e^{-ikR}}{R}\, dV_0 \qquad -(24)$$

except near $\theta_0 = \pi + \theta$

The position for eddies far from the edge is summarised schematically in Figure 3. Where equation 23 holds, the half-plane behaves like an infinite rigid plane with the edge having a negligible effect of order $(kr_0)^{-\frac{1}{2}}$ Where 24 holds, the sound is just that of an eddy in free turbulence, the edge again having a negligible effect of order $(kr_0)^{-\frac{1}{2}}$. Finally, an eddy in the geometrical shadow of the field point produces sound pressures lower than those from free turbulence by the factor $(kr_0)^{-\frac{1}{2}}$. Between each of these three regions there is a region where the sound pressures are intermediate between those of the neighbouring regions. There is no sharp discontinuity between, say, the regions from where reflected and direct sound is heard and that from where only direct sound is heard. However, the angular (θ_0) extent of these transition regions decreases with increasing distance of the eddy from the edge. The narrower this transition region, the sharper does the contrast between the sound heard from one region become with that from another.

If an eddy is supported by the half-plane and is on the same side of it as the field point, then there is a fourfold increase in the sound intensity at the field point: if the eddy is on the opposite side of the half-plane, then the intensity is reduced by the large factor and may be taken as zero. Lastly, if the eddy is far from both the edge and the half-plane (but not in the shadow region) then the intensity is the same as if the turbulence was unbounded. This is true even when there is reflected sound for then the travel time of the reflected sound is many eddy lifetimes longer than the travel time of the direct sound.

The essential point is that, except when the eddy lies in the geometrical shadow of the field point, a turbulent eddy far from the edge produces a sound of intensity comparable to that of an eddy in free turbulence.

1.4 The Effect of Motion of the Half Plane

Until now the half plane has been supposed perfectly rigid. However, it is possible to discuss the case of a half plane which is sufficiently limp that it cannot support any normal stress.

The Fourier transformed version of Lighthill's equation, our equation (3) now has to be solved subject to the condition that $p^* = 0$ on the half plane.

A formal solution of equation (3) is now

$$p^* = \int \left(\frac{\partial^2 \rho v_i v_j}{\partial y_i \partial y_j} \right)^* \tilde{G} \, dV \qquad -- (25)$$

where $(\nabla^2 + k^2)\tilde{G} = -4\pi\delta(\underline{x} - \underline{y})$

and $\tilde{G} = 0$ on the half plane.

Macdonald has shown that

$$\tilde{G} = \frac{e^{-i\pi/4}}{\sqrt{\pi}} \left\{ \frac{e^{-ikR}}{R} \int_{-\infty}^{u_R} e^{-iu^2} du - \frac{e^{-ikR'}}{R'} \int_{-\infty}^{u_{R'}} e^{-iu^2} du \right\}$$

where the symbols have their previous significance. The only difference between G and $\tilde{G}$ is the change of sign of the "image" part of G.

If the divergences are completed in (25) then

$$p^* = \int (\rho v_i v_j)^* \frac{\partial^2 \bar{G}}{\partial y_i \partial y_j} dV - \int \rho v_n^2 \frac{\partial \bar{G}}{\partial n} dS$$

The surface integral is to be evaluated over the mean position of the half plane. We may omit it from further discussion by observing that because only one differentiation of $\bar{G}$ is involved the integral will contain the factor $(2kr_0)^{-\frac{1}{2}}$ which means that when $2kr_0 << 1$ it is negligible compared to the terms containing $(2kr_0)^{-3/2}$. arising from the double differentiations of the volume integrals. On the other hand when the surface integral is negligible compared to the terms retained on the volume integral. The subsequent analysis is almost identical for that given for a rigid half plane.

For turbulence very near the edge we find

$$4\pi p^* = k^2 \frac{2e^{i\pi/4}}{\sqrt{\pi}} \sin\theta/2 \; (\sin\phi)^{\frac{1}{2}} \times$$

$$\int \left\{ \rho v_r^2 \sin\theta_0/2 - \rho v_\theta^2 \cos\theta_0/2 - 2\rho v_r v_\theta \cos\theta_0/2 \right\}^* \times$$

$$(2kr_0)^{-3/2} \frac{e^{-ikR}}{R} dV_0 \qquad \text{- - - -(26)}$$

This should be compared with equation (26) (11) . The only significant difference is the replacement of the directional factor $\cos\frac{\theta}{2}$ in (11) by $\sin\frac{\theta}{2}$.

Again, when the turbulence is far from the edge, the only difference from the rigid case is that any reflected sound has a change of phase of π .

With both the rigid and the pressure release half planes having essentially the same effect on the turbulence produced noise, it seems reasonable to conjecture that homogeneous half planes of intermediate properties also do so.

1.5 The Effect of Viscosity

The momentum equation for a viscous compressible fluid is

$$\frac{\partial \rho \underline{v}}{\partial t} + \rho \underline{v}.\nabla \underline{v} + \underline{v}(\nabla.\rho\underline{v}) = -\nabla p + \eta \nabla^2 \underline{v} + (\zeta + \tfrac{1}{3}\eta)\nabla(\nabla.v)$$

η and ζ are the first and second coefficients of viscosity (assumed constant throughout fluid).

Eliminating the term $\frac{\partial \rho \underline{v}}{\partial t}$ between this and the continuity equation we have

$$\frac{\partial^2 \rho}{\partial t^2} - c^2 \nabla^2 \rho = \nabla^2(p - c^2\rho) + \nabla.\nabla \rho \underline{v}\,\underline{v} - (\zeta + \tfrac{4}{3}\eta)\nabla.\nabla(\nabla.\underline{v})$$

or, if $p = c^2\rho$ and we take the generalised Fourier transform of both sides

$$(\nabla^2 + k^2)p^* = (\zeta + \tfrac{4}{3}\eta)\nabla.\nabla(\nabla.\underline{v}^*) - \nabla.\nabla(\rho\underline{v}\,\underline{v})^*$$

Thus the right hand side of our basic equation 3 is augmented with the term $(\zeta + \frac{4}{3}\eta)\nabla.\nabla(\nabla.\underline{v}^*)$.

Proceeding as before with the half plane taken to be rigid we find

$$4\pi p^* = \int (\rho v_i v_j)^* \frac{\partial^2 G}{\partial y_i \partial y_j} dV_0$$

$$+ (\zeta + \tfrac{4}{3}\eta) \int G \frac{\partial^2 v_n}{\partial n^2} dS$$

$$+ k^2 (\zeta + \tfrac{4}{3}\eta) \int \underline{v} \cdot \nabla G \, dV \quad \text{--- (27)}$$

The right hand side of equation 6 is now augmented by two further terms.

Dimensional reasoning allows us to state that the magnitudes of the three terms on the right of 27 are in the ratio

$$1 \quad : \quad \frac{(\zeta + \tfrac{4}{3}\eta)}{\rho U \delta} \qquad \frac{\zeta + \tfrac{4}{3}\eta}{\rho U \delta} (k\delta)^2$$

$$\approx \quad 1 \quad : \quad Re^{-1} \quad : \quad M^2 Re^{-1}$$

where R_e is a Reynolds number for a sound producing eddy, M equal to $k\delta$ is a typical Mach number associated with the eddy. R_e is always much greater than unity and so we conclude that viscous effects are negligible.

1.6 General Implications of the Theory

We have seen that eddies close to the edge of a half plane are much more powerful sources of sound than eddies far from the edge. The intensity at a farfield point of the sound from a single eddy near the edge is given approximately by the formula (15) which, if the directional factors are suppressed, can be written

$$I = \frac{k^4 \rho_0 U^4 \alpha^2 \sin^2 \bar{\theta}\; V^2}{\pi^3 c\, R^2\, (k\bar{r}_0)^3} \quad \text{--(28)}$$

The corresponding formula for an eddy far from the edge (not in the shadow region) is equivalent to that of an eddy in free space

$$I = \frac{k^4 \rho_0 U^4 \alpha^2 V^2}{32 \pi^2 c R^2} \quad \text{---(29)}$$

We are now in a position to estimate the scales of a surface in the critical case when the surface sound has an intensity comparable to that arising from the eddies near the edge. Larger surfaces than this critical size will be essentially unaffected by the edges while smaller surfaces will be dominated by the edge noise.

Comparing (28) and (29) we see that an eddy near the edge radiates an acoustic intensity equivalent to that of $\frac{32}{\pi} \times (k\bar{r}_0)^{-3}$ eddies in free space or a quarter this number of eddies in the boundary layer far from the edge. A minimum estimate of $\bar{r}_0$ is the correlation radius δ of the eddy, corresponding to an eddy centred on the edge. An eddy further from the edge will give rise to an intensity appreciably lower than this closest eddy because of the dependence of the intensity on the third power of the distance from the edge. For instance, a doubling of the effective distance of an eddy from the edge results in a 9db lowering of the intensity. Taking, however, δ as our estimate for $\bar{r}_0$ the edge region is equivalent, in sound generating ability, to the area within $\frac{16}{\pi}(k\delta)^{-3} \times 2\delta$ of the edge. Since $k\delta$ is of order πM the surfaces must have dimension normal to the edge in excess of $\frac{16}{\pi^4} M^{-3}\delta$, or, equivalently, $\frac{8}{\pi^5} M^{-2}$ acoustic wavelengths if the edge effect is to be other than dominant. This is necessarily a minimum estimate, for no account has been taken of the eddies farther from the edge than the closest eddy but still well within a wave-length of the edge, but it does show that if the fluid is water when M is seldom above 10^{-2} then to all intents and purposes the flow noise from a surface with an edge comes large enough for surface noise to be important.

A further consideration of some practical importance can be deduced from (28). The factor $\sin^2 \bar{\Theta}$ reduces the scattered noise from flows which pass obliquely over the edge. It is difficult to justify the transfer of results obtained for such an ideal surface as an infinitely thin, rigid half plane to surfaces which are encountered in the real world, but this does suggest that the noise from a hydroplane can be considerably reduced by giving it a swept wing profile. Marine propellers with greater curvature in the span-wise direction might be expected to generate less noise than those which have the span-wise direction more or less radial. The effect would be slight, however.

1.7 Summary and Conclusions

The presence of the edge of a half plane in a turbulent fluid results in a large increase in the noise generated by that fluid. The parameter which is important is the product $2k\bar{r}_0$, where $\bar{r}_0$ is the distance of the centre of the eddy from the edge. Eddies which satisfy the inequality $2k\bar{r}_0 \ll 1$ have the sound output of the quadrupoles associated with the fluid motion in a plane normal to the edge increased by the factor $(k\bar{r}_0)^{-3}$. There is no enhancement of the sound from the longitudinal quadrupoles with axes parallel to the edge: the rr, θr and $\theta\theta$ quadrupoles are the dominant sound sources. The sound intensity in the farfield from these sources depends upon the fifth power of a typical fluid velocity. The intensity has a directional dependence on $\cos^2\theta/2$ if the half plane is rigid and $\sin^2\theta/2$ if it is a pressure release surface.

If the eddies are far from the edge so that $(k\bar{r}_0)^{\frac{1}{2}} \gg 1$ then the farfield sound has the same features as would be predicted by geometrical acoustics. The edge does not produce any significant sound amplification.

PART II

2.0 Introduction

Gas bubbles have for a long time been recognised as sources of sound in liquids. The frequency of volume pulsations of a bubble was first calculated by Minnaert[18] and it was recognised that in these pulsations the bubble behaved like a simple oscillatory system with damping. In 1956 Strasberg[19] indicated the factors influencing the amplitude of the resulting sound pressures and described how they could be calculated for several excitation mechanisms, including the flow of a liquid containing entrained bubbles past an obstacle. In this part of the thesis this latter form of excitation will be re-examined. Unlike Strasberg, it is not assumed here that the bubble follows a fluid streamline.

In section 2.1 the equation of motion of a bubble is established first for a bubble in an arbitrary flow and then in a potential flow past a circular cylinder, with due account taken both of the acceleration drag and the viscous drag. It is assumed that the motion of the bubble is precisely equivalent to that of a weightless rigid sphere of the same volume and that the drag coefficient for bubble Reynold's numbers greater than unity is given by an empirical formula obtained by Zahm[16].

In section 2.2 the equations of motion are integrated numerically for various values of the parameters involved and it is shown that the larger the bubble radius for a fixed value for the cylinder radius the greater is the departure of the path from the fluid streamline along which the bubble was originally moving.

In section 2.3 the particular case of a bubble on the upstream fluid stagnation streamline is discussed. It is shown that for any given incoming bubble there exists a point on this streamline where the bubble will come to rest, but that oscillations about this point are not possible.

In section 2.4 the acoustic response of a bubble is obtained in terms of the fluctuating external pressure field felt by the bubble and in the next section this is used to obtain the sound pressures produced by a bubble flowing past a circular cylinder. For a bubble which does not appear to strike the cylinder the sound spectrum and waveform are similar to those found using Strasberg's assumption of motion along a streamline.

In section 2.6 the consequences of bubble disintegration and motion relative to the adjoining liquid are discussed. Large pressures are shown to occur on the disintegration of a bubble into small fragments compared to the original bubble. Fluctuations in the wake and boundary layer of a bubble are suggested as possible means of exciting resonance frequency sound.

The equation of Motion of a Bubble

(a) General Considerations

Consider a small rigid body free to move within a fluid which is in some arbitrary steady motion. We suppose that the body is much smaller than any length scale associated with the fluid motion and no account will be taken of the effect of gravity. If, to begin with, we also ignore the disturbance to the fluid due to the body, then we may assume that every fluid particle in the neighbourhood of the body experiences the same acceleration, $\underset{\sim}{f}$ say, corresponding to a uniform fall of pressure in the direction of $\underset{\sim}{f}$ given by $-\nabla p = \rho \underset{\sim}{f}$, where ρ is the density of the fluid. The body, subject to this uniform fall of pressure, experiences a force analagous to the buoyancy force of Archimedes' principle equal to $\rho V \underset{\sim}{f}$, where V is the volume of the body. However, because the densities of the fluid, ρ, and the body, ρ_1, differ, the acceleration of the body, $\underset{\sim}{f}_1$, will not be the same as that of the fluid. The motion of the body relative to the fluid causes the fluid to acquire some additional motion. There will now be two further forces acting on the body: an acceleration drag equal to the product of the added mass, $\rho V'$ say, of the body and the relative acceleration of the body and a viscous drag due to the formation of a boundary layer on, and a wake behind, the body. If we now equate the resultant of these forces acting on the body to the product of the mass of the body and its acceleration then we have

$$\rho_1 V \underset{\sim}{f_1} = \rho V \underset{\sim}{f} - \rho V'(\underset{\sim}{f_1} - \underset{\sim}{f}) - \underset{\sim}{D}$$

That is,

$$\underset{\sim}{f_1} = \frac{\rho(V + V')}{\rho_1 V + \rho V'} \underset{\sim}{f} - \frac{1}{\rho_1 V + \rho V'} \underset{\sim}{D} \quad \text{---(30)}$$

We now make the assumption that the motion of a bubble in a liquid is the same as that of a rigid weightless sphere of equal volume. It has been known for some time (see Peebles and Garbor [14] for references) that unless special efforts are made to have pure water the drag coefficient for bubbles rising under gravity in water closely approximates that of a rigid sphere of the same volume, at least for Reynold's numbers (based on velocity of rise and equivalent spherical diameter) up to about 200. This rather surprising effect is usually attributed to a monomolecular layer of surfactants surrounding the bubble which resist changes in bubble shape. Even though a bubble may have the same drag as a rigid sphere at up to quite high Reynold's numbers, a bubble is noticeably non-spherical at Reynold's numbers of order one. The added mass of the bubble depends on the bubble shape but under our basic assumption we do not take this into account. A further complication associated with the added mass is that even for a sphere the added mass equals $\frac{1}{2}\rho V$ only in the absence of any other bodies in the flow. An alternative approach to that which led to equation 30 and which does not suffer from this last difficulty and which, in principle, allows an estimate to be made of how close a sphere may approach another body before departures of the added mass from $\frac{1}{2}\rho V$ become significant, is provided by the Landweber and Yih [15] formula for the force on an immersed body in the presence of other bodies. In practice, however, even for the case of one sphere in the presence of another, this formula quickly becomes unworkable. If, in the two sphere problem, only the terms which contain the radius of the smaller sphere to the third power are retained, the Landweber and Yih formula reduces to equation 30 with V' set equal to $\frac{1}{2}V$ and $\underset{\sim}{D}$ put equal to zero. It can be shown that if a is the radius of the moving sphere, b the radius of the fixed sphere and c the distance between the centres of the spheres, then the ratio of the largest term neglected to the smallest retained is $\frac{a^3c}{(c - b^2/c)^4}$. If n a is closest the centre of the moving sphere approaches the surface of the fixed sphere, and m a is the smallest value of c attained then the largest value of this ratio is $\frac{m}{16n^4}$. For example, if m = 500, n = 5 this ratio has the value 0.05. We might expect similar results for a sphere nearing other bodies so that equation 30 should hold for bubbles farther than a few (say five) bubble radii from any surface with V' set equal to $\frac{1}{2}V$.

The remaining question to be settled before equation 30 is applied to a bubble is the dependence of $\underset{\sim}{D}$ on the flow parameters. We write

$$\underset{\sim}{D} = C_D \, \tfrac{1}{2}\rho(\underset{\sim}{u}_1 - \underset{\sim}{u})^2 \pi a^2 \, \frac{\underset{\sim}{u}_1 - \underset{\sim}{u}}{|\underset{\sim}{u}_1 - \underset{\sim}{u}|}$$

where $\underset{\sim}{u}$, $\underset{\sim}{u}_1$ are the velocities of the liquid and bubble respectively, a is the equivalent spherical radius of the bubble and C_D is the drag coefficient.

For Reynold's numbers (defined by Re = $\frac{2|\underset{\sim}{u}_1 - \underset{\sim}{u}|a}{\nu}$) less than about 2 the Stokes-Oseen relation for C_D for a solid sphere agrees well with the experimentally determined values but for much larger Reynold's numbers there is no theoretical formula for C_D.

We shall take

$$C_D = \frac{24}{R_e} + 4.5 \qquad \text{when } R_e < 1$$

and

$$C_D = \frac{28}{R_e^{0.85}} + 0.48 \qquad \text{when } R_e \geq 1$$

The first expression is due to Stokes and Oseen and the second is an empirical formula found by Zahm[16] to give reasonable agreement with experiment within the range

$$0.2 < R_e < 200,000$$

We are now in a position to write down the equation of motion of a bubble under the assumptions that it is the same as that for a rigid weightless sphere, that the bubble is not too near any surface and that the viscous drag on the bubble is the same as that for a rigid sphere. It is

$$\underset{\sim}{f_1} = 3\underset{\sim}{f} - \frac{3}{4}\frac{C_D}{a}\,|\underline{u}_1 - \underline{u}|\,(\underline{u}_1 - \underline{u})$$

$$= 3\underline{f} - \frac{3}{4a}\left(\frac{12\nu}{a} + \frac{9}{2}|\underline{u}_1 - \underline{u}|\right)(\underline{u}_1 - \underline{u})$$

$$\text{if } R_e = \frac{2a|\underline{u}_1 - \underline{u}|}{\nu} < 1$$

$$= 3\underline{f} - \frac{3}{4a}\left(28\left(\frac{\nu}{2a}\right)^{0.85}|\underline{u}_1 - \underline{u}|^{0.15} + 0.48|\underline{u}_1 - \underline{u}|\right)\times(\underline{u}_1 - \underline{u})$$

$$\text{if} \quad R_e \geq 1 \qquad ---(31)$$

(b) <u>The Equation of Motion of a Bubble in a Flow Part of a Circular Cylinder</u>

We now apply this last equation to a bubble entrained in a steady uniform irrotational flow about a circular cylinder of radius R. Choosing a cartesian set of axes with z axis along the axis of the cylinder and x axis in the direction of the uniform stream, it can be readily shown that the fluid at the point (x, y) has acceleration

$$\underline{f} = (f_x, f_y) = \frac{2U^2R^2}{(x^2+y^2)^3}\left\{x(x^2-3y^2-R^2),\ y(3x^2-y^2-R^2)\right\}$$

and velocity

$$\underline{u} = (u_x, u_y) = U\left\{1 - \frac{(x^2-y^2)R^2}{(x^2+y^2)^2},\ \frac{-2xyR^2}{(x^2+y^2)^2}\right\}$$

Here U is the velocity of the fluid far from the cylinder. If now

$$\underset{\sim}{f}_1 = \left(\frac{d^2x}{dt^2}, \frac{d^2y}{dt^2} \right)$$

and

$$\underset{\sim}{u}_1 = \left(\frac{dx}{dt}, \frac{dy}{dt} \right)$$

then for $R_e < 1$

$$\frac{d^2x}{dt^2} = \frac{6U^2R^2x(x^2-3y^2-R^2)}{(x^2+y^2)^3}$$

$$- \frac{1}{a}\left(\frac{9\nu}{a} + \frac{27}{8}|\underset{\sim}{u}_1 - \underset{\sim}{u}| \right)\left(\frac{dx}{dt} - U\left(1 - \frac{x^2-y^2}{(x^2+y^2)^2}\right)\right)$$

and

$$\frac{d^2y}{dt^2} = \frac{6U^2R^2y(3x^2-y^2-R^2)}{(x^2+y^2)^3}$$

$$-\frac{1}{a}\left(\frac{9\nu}{a} + \frac{27}{8}|\underset{\sim}{u}_1 - \underset{\sim}{u}| \right)\left(\frac{dy}{dt} + \frac{2UxyR^2}{(x^2+y^2)^3} \right)$$

where

$$|\underset{\sim}{u}_1 - \underset{\sim}{u}| = \left\{ \left(\frac{dx}{dt} - u_x \right)^2 + \left(\frac{dy}{dt} - u_y \right)^2 \right\}^{\frac{1}{2}}$$

while if $R_e \geq 1$

$$\frac{d^2x}{dt^2} = \frac{6U^2R^2x(x^2-3y^2-R^2)}{(x^2+y^2)^3}$$

$$-\frac{3}{4}\left(28\left(\frac{D}{2a}\right)^{0.85}\left|\underline{u}_1-\underline{u}\right|^{0.15}+0.48\left|\underline{u}_1-\underline{u}\right|\right)$$

$$\times\left(\frac{dx}{dt} - U\left(1-\frac{(x^2-y^2)R^2}{(x^2+y^2)^2}\right)\right)$$

and

$$\frac{d^2y}{dt^2} = \frac{6U^2R^2y(3x^2-y^2-R^2)}{(x^2+y^2)^3}$$

$$-\frac{3}{4a}\left(28\left(\frac{D}{2a}\right)^{0.85}\left|\underline{u}_1-\underline{u}\right|^{0.15}+0.48\left|\underline{u}_1-\underline{u}\right|\right)$$

$$\times\left(\frac{dy}{dt} + \frac{2UxyR^2}{(x^2+y^2)^2}\right)$$

Changing to dimensionless variables by setting $x = Rx'$, $y = Ry'$ and $t = \frac{R}{U}t'$ and then dropping the dashes we have

$$\frac{d^2x}{dt^2} = \frac{6x(x^2-3y^2-1)}{(x^2+y^2)^3}$$

$$-\frac{R}{a}\left(\frac{18}{r_e}+\frac{27}{8}\left|\underline{u}_1-\underline{u}\right|\right)\left(\frac{dx}{dt}-\left(1-\frac{x^2-y^2}{(x^2+y^2)^2}\right)\right) \quad \text{---(32a)}$$

and

$$\frac{d^2y}{dt^2} = \frac{6y(3x^2 - y^2 - 1)}{(x^2+y^2)^3}$$

$$-\frac{R}{a}\left(\frac{18}{r_e} + \frac{27}{8}\left|\underline{u}_1 - \underline{u}\right|\right)\left(\frac{dy}{dt} + \frac{2xy}{(x^2+y^2)^2}\right) \qquad --(32\ b)$$

when $r_e \left|\underline{u}_1 - \underline{u}\right| < 1$

and

$$\frac{d^2x}{dt^2} = \frac{6x(x^2 - 3y^2 - 1)}{(x^2+y^2)^3}$$

$$- \frac{3R}{4a}\left(\frac{28}{r_e^{0.85}}\left|\underline{u}_1 - \underline{u}\right|^{0.15} + 0.48\left|\underline{u}_1 - \underline{u}\right|\right)$$

$$\times\left(\frac{dx}{dt} - \left(1 - \frac{x^2-y^2}{(x^2+y^2)^2}\right)\right) \qquad -(32\,c)$$

and

$$\frac{d^2y}{dt^2} = \frac{6y(3x^2 - y^2 - 1)}{(x^2+y^2)^3}$$

$$-\frac{R}{a}\frac{3}{4}\left(28(r_e)^{-0.85}\left|\underline{u}_1 - \underline{u}\right|^{0.15} + 0.48\left|\underline{u}_1 - \underline{u}\right|\right)$$

$$\times\left(\frac{dx}{dt} + \frac{2xy}{(x^2+y^2)^2}\right) \qquad ---(32\ d)$$

when $\quad r_e \left| \underline{u}_1 - \underline{u} \right| \geq 1$

Here $\quad r_e = \frac{2aU}{\nu}$

and

$$\left| \underline{u}_1 - \underline{u} \right| = \left\{ \left(\frac{dx}{dt} - \left(1 - \frac{x^2 - y^2}{(x^2+y^2)^2} \right) \right)^2 + \left(\frac{dy}{dt} + \frac{2xy}{(x^2+y^2)^2} \right)^2 \right\}^{\frac{1}{2}}$$

The Bubble Path

Equations 32 were integrated numerically for various values of the parameters R/a and r_e and for different initial conditions. The fourth order Runge-Kutta method was employed and the actual computations carried out on Imperial College's IBM 1794 computer.

It will be recalled that at each integration step the Runge-Kutta method advances the solution of a differential equation from its previously given or calculated values to values found by calculating the sum of the first five terms of the Taylor series which represents the solution. It is necessary, of course, that the sum of the first five terms be a good approximation to the sum of the complete series and this can always be ensured by choosing a suitably small step length.

Now for a given step length the error inherent in this method of integration will be greatest when

is sufficiently large for equations 32c or 32d to be effectively of the form
$\frac{d^2x}{dt^2} = -\alpha\left(\frac{dx}{dt} - h\right)^2$, for some constants α, h.
Such an equation has the solution

$$x = x_0 + ht + \frac{1}{\alpha}\log\left(1 + (u_0 - h)\alpha t\right)$$

when, at $t = 0$ $x = x_0$ and $\frac{dx}{dt} = u_0$

Clearly, when equations 32c or 32 d are in this form the step length, Δt, must be such that

$$(u_0 - h)\alpha\ \Delta t < 1$$

In the actual integration of equations 32 the step length was continually changed so that
$|u_1 - u| \times 0.36\frac{R}{a} \times \Delta t$ was always less than 0.1. With this step length control the error at each step in the integration should be less than one thousandth of the magnitude of the second term of the Taylor series representing the solution at the beginning of each integration step. The largest value of Δt employed was 0.1 which, in the absence of the drag terms, would cause an error at each step of order 10^{-5}.

Appendix A contains a typical programme listing.

Fig. 4 is a computer "Calcomp" plot of the bubble trajectories obtained by integrating equations 32 for bubbles initially moving with the liquid (taken here and in all further computations to be water) when 20 cylinder radii upstream and at various distances from the fluid stagnation streamline. The bubble and cylinder radii were 0.1 and 10 cms respectively and the uniform stream velocity was taken to be 5 metres per second. The broken curves show the fluid streamlines along which the bubbles were originally moving. These streamlines were computed by integrating equations 32 when the multiplier '6' on the right hand side of each equation was replaced by '2' and the viscous drag terms set equal to zero.

It can be seen that upstream of the cylinder the bubbles are displaced off the streamlines on which they were originally moving in a direction away from the cylinder but that near the cylinder the bubbles move within the original streamlines, some of them actually striking the cylinder.* However, as our basic equation of motion no longer holds for bubbles very near the cylinder this cannot be taken as evidence of actual collisions with the cylinder. We can show though that when a bubble is close enough to the cylinder for the

*The short lines within the cylinder indicate where the solutions of 32 intersect the cylinder.

cylinder to appear locally plane (equations 32 will now not hold) then, ignoring viscous forces, the bubble will experience a force directed towards the cylinder. Thus, provided again that the bubble is not too near the surface, the kinetic energy of a system consisting of a rigid weightless spherical bubble moving in a fluid bounded by a fixed rigid wall is given by

$$T = \tfrac{1}{2}(A\dot{\xi}^2 + B\dot{\eta}^2). \qquad \text{--- } 33$$

where (ξ, η) are the coordinates of the centre of the sphere referred cartesian axes $O\xi$ perpendicular to the wall and $O\eta$ parallel to the wall, and where

$$A = \tfrac{2}{3}\pi\rho a^3\left(1 + \tfrac{3}{8}\,a^3/\xi^3\right)$$

$$B = \tfrac{2}{3}\pi\rho a^3\left(1 + \tfrac{3}{16}\,a^3/\xi^3\right)$$

(see Milne Thompson [17], section 12.61, for proof)

In the absence of any external forces Lagrange's equations now lead to the following equations of motion for the bubble

$$0 = \left(1 + \tfrac{3}{8}\,a^3/\xi^3\right)\ddot{\xi} + \tfrac{9}{32}\,a^3/\xi^4\left(\dot{\eta}^2 - 2\dot{\xi}^2\right)$$

and

$$0 = \frac{d}{dt}\left[\left(1 + \frac{3}{16}\,a^3/\xi^3\right)\dot{\eta}\right]$$

From the first of these we see that if $\dot{\eta}^2 > 2\dot{\xi}^2$ that is, if the angle of incidence of the bubble on the surface (0° equals normal incidence) is greater than about 55° - then in the region where equation 33 holds, the bubble will be urged towards the cylinder. We might expect the viscous drag on the bubble would tend to give high angles of incidence. This does not of course prove that a bubble will hit the cylinder and only suggests that in a certain region near the surface where our basic equation of motion is no longer valid the bubble can still be moving towards the surface.

Whether or not some bubbles do in fact hit the surface, their subsequent fate is likely to be just the same - namely, disintegration into smaller bubbles. For example, in Figure 4 the bubble originally on the streamline 0.2 cylinder radii off the stagnation streamline has a normal velocity of approach to the cylinder of approximately $0.5\,U$ when seven bubble radii from the cylinder, i.e., in a region where our basic equation is valid. Either way, if the bubble hits the cylinder or is repelled before actually coming into contact the bubble must experience a deceleration of <u>at least</u> 2.25g. If the region of deceleration is much less than seven bubble radii the deceleration is correspondingly the greater. Bubble disintegration would be expected if the inertia (density times acceleration) of the fluid at the bubble wall greatly exceeded the surface tension pressure within the bubble. The acoustical consequences of a bubble disintegration will be considered in a later section.

Figure 5 is a plot of some bubble trajectories for a case which is at the limits of the validity of the basic equation of motion. Here $R/a = 10$ and $R_e = 10^5$ and now it is no longer true to regard the pressure field around the bubble as being constant over the surface of the bubble although this is in fact done.

The bubble paths, as might have been expected, show larger departures from the fluid streamlines than those of Figure 4 when R/a was equal to 100. Perhaps the most interesting feature of Figure 5 is the very large divergence of some of the paths downstream of the cylinder. This will have an important effect on the bubble density downstream of the cylinder and this will be discussed in section

(In the figure, the fluid streamlines are truncated at the points where, under the assumption that the bubble was constrained to move along the streamline, the bubble would strike the cylinder.)

Figure 6 shows the bubble paths for a bubble

FIGURE 4: Bubble Paths.

$$\begin{cases} R = 10 \text{ cms.} \\ a = 0.1 \text{ cms.} \\ U = 5 \text{ metres/sec.} \end{cases}$$

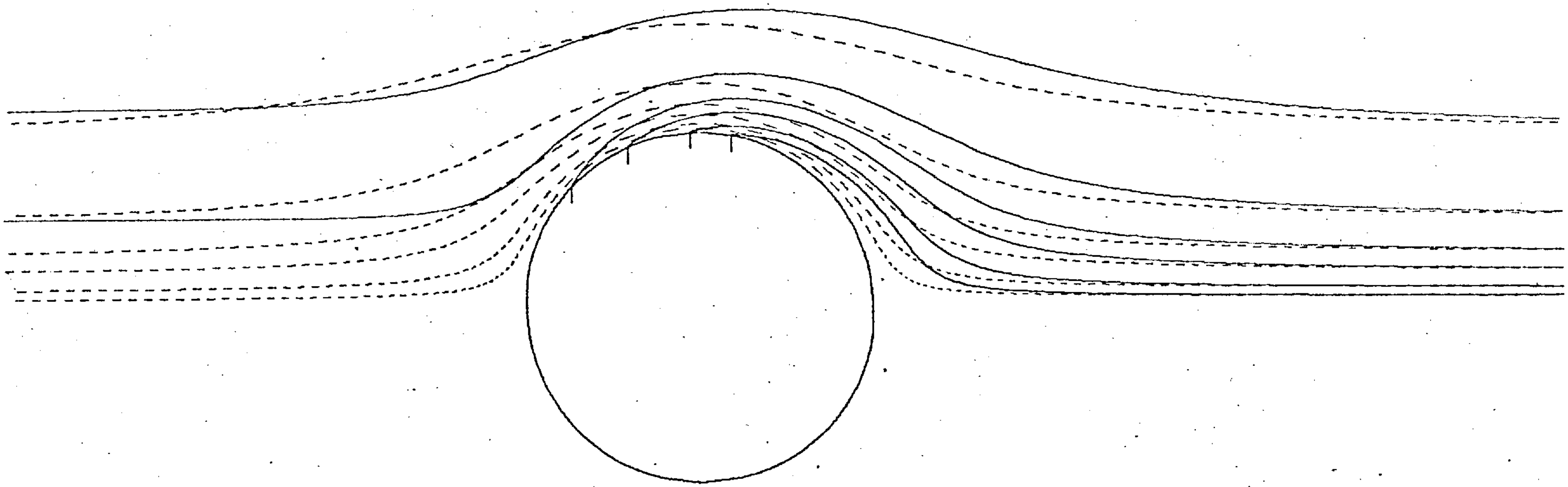

FIGURE 5: Bubble Paths.

R = 10 cms.
a : 1·0 cms.
U = 5 metres/sec.

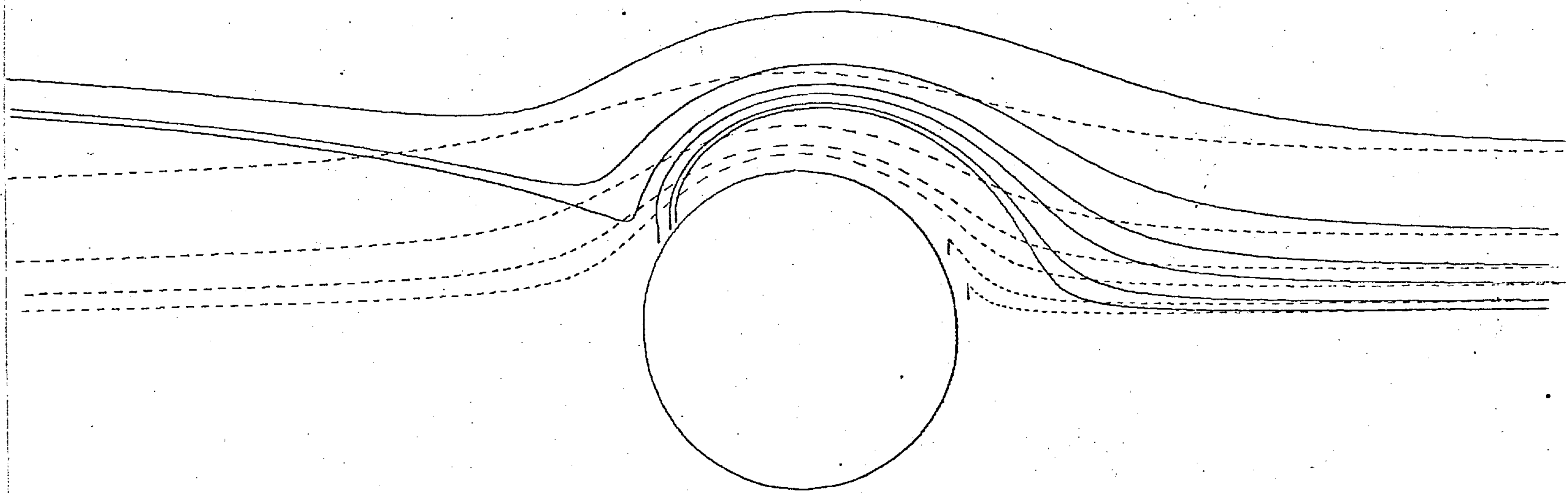

FIGURE 6: Bubble Paths for various $\frac{R}{a}$.

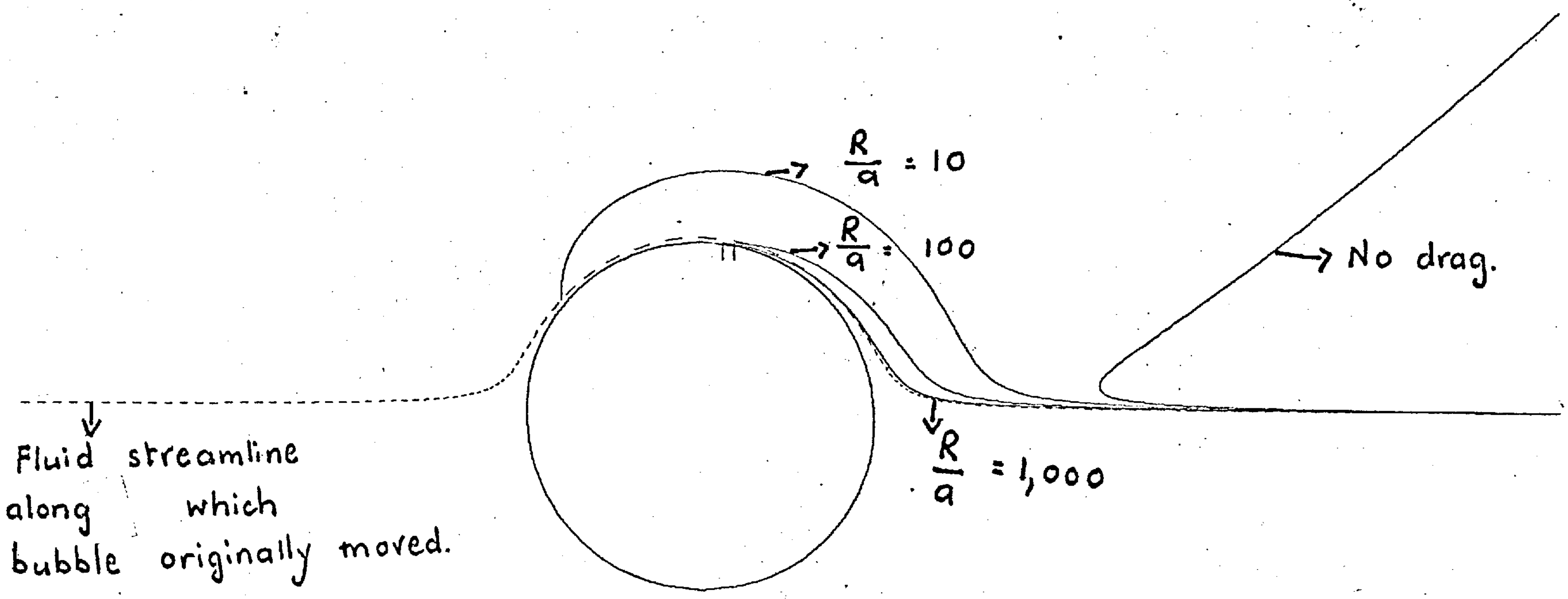

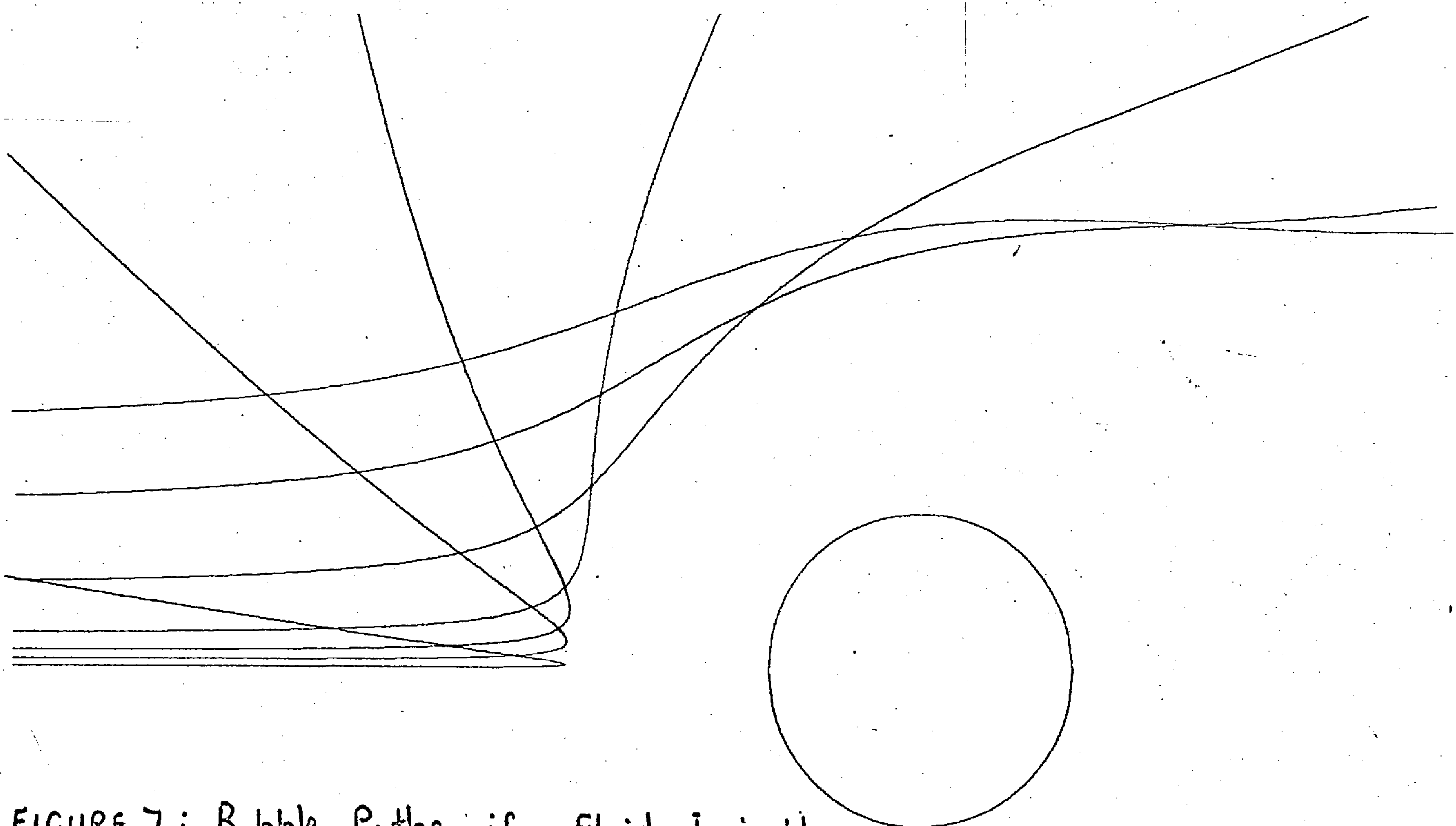

FIGURE 7: Bubble Paths if Fluid Inviscid.

initially 0.05 bubble radii off the stagnation streamline and again initially moving with the fluid. Γ_e was held constant (at 10^4) but R/a allowed to vary. When R/a = 1000 there is little departure from the fluid streamline but what there is is enough for the bubble to "hit" the cylinder. The bubble path obtained when there is assumed to be no viscous drag emphasised the leading role played by the drag force. This is further demonstrated in Figure 7 which shows more paths in an inviscid fluid. It would be difficult to imagine a greater discrepancy from the fluid streamlines.

The qualitative features of this diagram may be understood if the bubble is regarded as a smooth sphere rolling under the influence of gravity on a smooth surface with height contours proportional to three times the pressure contours around the cylinder. The motion of such a sphere depends on its initial velocity: the greater the initial velocity the higher up the hill it ascends before rolling back. Similarly the motion of a bubble in an inviscid fluid likewise depends critically on the initial velocity: if the bubble is placed at rest near the stagnation streamline it will move in (roughly) the opposite direction to the fluid: if it is initially projected along a fluid streamline with $\sqrt{3}$ times the velocity of the fluid at its initial position it will remain on the streamline but its velocity will always be $\sqrt{3}$ times that of the fluid.

(This last because, using the previous notation, the equations of motion of the bubble are

$$\frac{d^2x}{dt^2} = 3f_x \quad \text{and} \quad \frac{d^2y}{dt^2} = 3f_y \ .$$

Make the substitution $t' = \sqrt{3}\,t$.

Then $\dfrac{d^2x}{dt'^2} = f_x$ and $\dfrac{d^2y}{dt'^2} = f_y$

But these are just the equations of motion of a fluid particle in a potential flow about the cylinder. An integral of these equations is then

$$\frac{dx}{dt'} = u_x \quad \text{and} \quad \frac{dy}{dt} = u_y$$

That is, $\dfrac{dx}{dt} = \sqrt{3}\,u_x$ and $\dfrac{dy}{dt'} = \sqrt{3}\,u_y$
and this will be the first integral of the equations of motion of the bubble if the bubble is initially moving with $\sqrt{3}$ times the local velocity of the fluid.)

If the fluid is viscous, however, the motion of a bubble is effectively independent of its initial velocity. Thus if the bubble is initially projected with velocity v_0 where the fluid has velocity V the initial motion of the bubble is governed by an equation of the form

$$\frac{d^2x}{dt^2} = -\alpha\left(\frac{dx}{dt} - V\right)^2$$

which has the integral

$$\frac{dx}{dt} = V + (v_0 - V)e^{-\alpha(x - Vt - x_0)}$$

α is of order R/a , so that unless ($v_0 - V$) is very large (when the bubble is certain to disintegrate), the velocity of the bubble is very rapidly that of the fluid.

It is obvious from Figure 7 that the velocity of bubbles in an inviscid fluid cannot in general be derived from a simple velocity potential. If the oncoming fluid stream at large distances from the cylinder contains a uniform density of bubbles then this will mean that near the cylinder this bubble density will cease to be constant. The motion of a bubble in a viscous fluid is forced by the same pressure field as a bubble in an inviscid fluid with viscous drag having the essentially negative role of resisting relative motion between the bubble and the fluid. Accordingly we would not expect the velocity of a bubble in a viscous flow to be solenoidal.

Bubble on the Stagnation Streamline

On the stagnation streamline the net force on a bubble due to the pressure field around the cylinder is collinear with the viscous drag. We now investigate the possibility that there be a point upstream of the cylinder where a bubble initially at rest will remain at rest because the two forces are equal and opposite.

The equation of motion of a bubble on the stagnation streamline is

$$\frac{d^2x}{dt^2} = \frac{6(x^2-1)}{x^5} + \frac{R}{a}\left(\frac{18}{r_e} + \frac{27}{8}\left(1-\frac{1}{x^2}-\frac{dx}{dt}\right)\right) \times \left(1-\frac{1}{x^2}-\frac{dx}{dt}\right)$$

if $\quad r_e\left(1-\frac{1}{x^2}-\frac{dx}{dt}\right) < 1$

and

$$\frac{d^2x}{dt^2} = \frac{6(x^2-1)}{x^5} + \frac{3}{4}\frac{R}{a}\left\{\frac{28}{r_e^{0.85}}\left(1-\frac{1}{x^2}-\frac{dx}{dt}\right)^{0.15} + 0.48\left(1-\frac{1}{x^2}-\frac{dx}{dt}\right)\right\}\left(1-\frac{1}{x^2}-\frac{dx}{dt}\right)$$

$- \text{Eq}^{\text{tn}}\ 34$

if $\quad r_e\left(1 - \frac{1}{x^2} - \frac{dx}{dt}\right) \geq 1$.

where it has been assumed that $\frac{dx}{dt} \leq 1 - \frac{1}{x^2}$ which will certainly be the case if the bubble was once moving with the fluid. A bubble placed at rest at the point $x = x_0$ will remain there if either

$$0 = \frac{6(x_0^2 - 1)}{x_0^5} + \frac{R}{a}\left(\frac{18}{r_e} + \frac{27}{8}\left(1 - \frac{1}{x_0^2}\right)\right)\left(1 - \frac{1}{x_0^2}\right)$$

or

$$0 = \frac{6(x_0^2 - 1)}{x_0^5} + \frac{3R}{4a}\left(\frac{28}{r_e^{0.85}}\left(1 - \frac{1}{x_0^2}\right)^{0.15} + 0.48\left(1 - \frac{1}{x_0^2}\right)\right) \times \times \left(1 - \frac{1}{x_0^2}\right)$$

depending on whether $r_e\left(1 - \frac{1}{x_0^2}\right)$ is or is not smaller than unity.

That is, if

$$0 = \frac{x_0^2 - 1}{x_0^5}\left(6 + \frac{R}{a}\left(\frac{18}{r_e} + \frac{27}{8}\left(1 - \frac{1}{x_0^2}\right)\right)x_0^3\right)$$

or

$$0 = \frac{x_0^2 - 1}{x_0^5}\left(6 + \frac{3R}{4a}\left(\frac{28}{r_e^{0.85}}\left(1 - \frac{1}{x_0^2}\right)^{0.15} + 0.48\left(1 - \frac{1}{x_0^2}\right)\right)x_0^3\right)$$

It is clear that for each of these equations there is a finite real root less than -1.

The question now arises: if the bubble is given a small displacement from x_0 along the streamline, will the bubble oscillate about x_0 ? Were it to do so there would be the possibility of sound both from the coupling of the radial oscillations of the bubble with the lateral oscillations of the bubble and from the bubble, now regarded as a rigid sphere, radiating as a dipole source.

We consider the two cases of $r_e\left(1-\frac{1}{x_0^2}\right)$ very much smaller and much greater than unity.

$\underline{r_e\left(1-\frac{1}{x_0^2}\right) << 1}$

The equation of motion is

$$\frac{d^2x}{dt^2} = \frac{6(x^2-1)}{x^5} + \frac{R}{a}\frac{18}{r_e}\left(1-\frac{1}{x^2}-\frac{dx}{dt}\right)$$

x_0 is the solution of $0 = 1 + \dfrac{R}{a}\dfrac{3}{r_e}x_0^3$

where we require $\dfrac{a}{R}\dfrac{r_e}{3}$ to be greater than 1.

Writing $x = x_0 + x'$ in the equation of motion and expanding the righthand side we have

$$\frac{d^2x'}{dt^2} = \left\{\frac{30-18x_0^2}{x_0^6} + \frac{R}{a}\frac{36}{r_e}\frac{1}{x_0^3}\right\}x' - \frac{R}{a}\frac{18}{r_e}\frac{dx'}{dt}$$

+ higher powers of x' and $\dfrac{dx'}{dt}$ which we discard.

or $$\frac{d^2x'}{dt^2} = \frac{18(1-x_o^2)}{x_o^6}x' + \frac{6}{x_o^3}\frac{dx'}{dt}$$

after a little manipulation. This is the equation of a damped S.H.M. oscillator but it will not have an oscillatory solution because $\left(\frac{3}{x_o^3}\right)^2 - \frac{18(1-x_o^2)}{x_o^6} = \frac{18x_o^2-9}{x_o^6}$ is necessarily positive.

$\underline{r_e\left(1-\frac{1}{x_o^2}\right) >> 1}$

The equation of motion is

$$\frac{d^2x}{dt^2} = \frac{6(x^2-1)}{x^5} + \frac{0.36R}{a}\left(1-\frac{1}{x^2}-\frac{dx}{dt}\right)^2$$

and x_o is the solution of

$$6 + 0.36\frac{R}{a}x_o(x_o^2-1) = 0 .$$

Setting $x = x_o + x'$, the equation of motion becomes, after a little manipulation

$$\frac{d^2x'}{dt^2} + \frac{12}{x_o^3}\frac{dx'}{dt} + \frac{6(1-x_o^2)}{x_o^6}x' = 0$$

Again there will be no oscillatory solution because

$\left(\frac{6}{x_o}\right)^3 - \frac{6(1-x_o^2)}{x_o^6} = \frac{30+6x_o^2}{x_o^6}$ is necessarily positive.

Thus in both cases the bubble returns to x_o in a manner typical of an "over-damped" oscillator. An incoming bubble will become trapped by this system and ultimately come to rest at x_o .

For intermediate values of $r_E\left(1-\frac{1}{x_o^2}\right)$ it can be shown using the same approach as above that the same conclusions still hold. The working is necessarily more clumsy and will not be given here.

In a computer experiment a bubble initially 10 cylinder radii upstream and for which R/a = 100 and r_e = 10^4 approached monotonically the value of x_o (-1.0656) calculated separately as the root of equation 34d. In 15 dimensionless time intervals after being at the point (10, 0) the bubble was at the point -1.0670 and moving with a velocity of less than 0.003. By comparison, the same bubble constrained to move with the fluid ~~and~~ came within one bubble radii of the cylinder after 11.5 time intervals.

Acoustic Response of a Spherical Bubble to an Applied Pressure Field.

Consider a spherical bubble of internal pressure P and radius a within a liquid which exerts on it the pressure Pa, assumed to have no spatial variation over regions comparable to the bubble. A change in this ambient pressure causes both a change in the internal pressure of the bubble and a change in its radius. The liquid surrounding the bubble is set in motion creating a pressure field within the liquid which is propagated out from the bubble at the speed of sound. At the distance r from the centre of the bubble this pressure is of the form

$$p(r,t) = \frac{Q(t - r/c)}{r}$$

where $Q(t)$ is the (as yet unknown) acoustic strength of the bubble and c is the speed of sound in the liquid.

Near the bubble the momentum equation for the liquid (assumed inviscid) is

$$\rho \frac{dv}{dt} + \frac{\partial p}{\partial r} = 0$$

where v is the (radial) velocity of the liquid and ρ is its density.

That is, $\rho \dfrac{dv}{dt} - \dfrac{p(r, t - r/c)}{r} - \dfrac{1}{c} \dfrac{\partial p(r, t - r/c)}{\partial t} = 0.$

At the bubble surface the acceleration of a liquid particle is $\dfrac{d^2 a}{dt^2}$ so on setting r equal to a this last equation becomes

$$\rho \frac{d^2 a}{dt^2} = \frac{p(a, t - a/c)}{a} + \frac{1}{c} \frac{\partial p}{\partial t}(a, t - a/c)$$

If we now assume that the bubble radius is very much less than a typical wavelength of the sound produced by the bubble we may write this

$$\rho \frac{d^2 a}{dt^2} = \frac{p(a, t)}{a} + \frac{1}{c} \frac{\partial p(a, t)}{\partial t} \qquad -(35)$$

The equation of state for the gas within the bubble is Pa^{38} = const, where γ is equal to the ratio of the specific heats of the gas if the pressure changes within the bubble are sufficiently rapid for there to be negligible heat flow across the surface of the bubble and is equal to unity if the gas remains in thermal equilibrium with the surrounding fluid.

Logarithmic time differentiation of the equation of state yields

$$\frac{1}{P} \frac{dP}{dt} + \frac{3\gamma}{a} \frac{da}{dt} = 0 \quad ,$$

which on further differentiation gives the equation

$$\frac{d^2P}{dt^2} + \frac{3\gamma}{a}\frac{dP}{dt}\frac{da}{dt} + \frac{3\gamma}{a}P\frac{d^2a}{dt^2} - \frac{3\gamma}{a^2}P\left(\frac{da}{dt}\right)^2 = 0 .$$

Omitting the non-linear terms we have

$$\frac{d^2P}{dt^2} + \frac{3\gamma P}{a}\frac{d^2a}{dt^2} = 0 \quad \ldots (36)$$

Finally, equating the normal stresses at the surface of the bubble,

$$P = P_a + p(a,t) + \frac{2\sigma}{a} \quad --(37)$$

where $\frac{2\sigma}{a}$ is the surface tension pressure. Differentiating twice with respect to time and again omitting the non-linear terms, we have

$$\frac{d^2P}{dt^2} = \frac{d^2P_a}{dt^2} + \frac{\partial^2 p(a,t)}{\partial t^2} - \frac{2\sigma}{a}\frac{d^2a}{dt^2} \quad --(38)$$

Eliminating $\frac{d^2P}{dt^2}$ and $\frac{d^2a}{dt}$ between equations 35, 36 and 37 we find

$$\frac{\partial^2 p}{\partial t^2} + \left\{\frac{3\gamma P}{\rho c a} - \frac{2\sigma}{a^2\rho c}\right\}\frac{\partial p}{\partial t} + \left\{\frac{3\gamma P}{a^2\rho} - \frac{2\sigma}{\rho a^3}\right\}p = -\frac{d^2P_a}{dt^2}$$

For a water/air interface $\sigma \approx$ 80 dynes/cm, and P is at least one atmosphere, or 10^6 dynes/cm^2, so that except for very small bubbles (a $\approx 10^{-4}$ cm) the terms involving σ may be omitted. We shall suppose this is always possible. Thus

$$\frac{\partial^2 p}{\partial t^2} + \frac{3\gamma P}{\rho c a}\frac{\partial p}{\partial t} + \frac{3\gamma P}{a^2 \rho} p = -\frac{d^2 P_a}{dt^2} \quad \text{-- (39)}$$

an equation connecting the acoustic pressure at the bubble surface to changes in the ambient pressure.

For brevity we set $2B = \dfrac{3\gamma P}{\rho c a}$, $\omega_0^2 = \dfrac{3\gamma P}{a^2 \rho}$

For an air bubble in water with an internal pressure of one atmosphere and radius 0.1 cm,

$$2B = 2.8 \times 10^2 \text{ sec}^{-1}, \quad \omega_0^2 = 4.2 \times 10^8 \text{ sec}^{-2}$$

$$(\gamma = 1.4)$$

The sound pressure at a distance r from the bubble is related to $p(a,t)$ by

$$p(r,t) = \frac{a}{r}\, p(a, t - r/c) \quad \text{---(40)}$$

Defining the Fourier transform of the acoustic wall pressure as

$$p^*(a,\omega) = \frac{1}{2\pi}\int_{-\infty}^{\infty} p(a,t)\, e^{-i\omega t}\, dt$$

then, taking the Fourier transform of equation we have

$$(-\omega^2 + \omega_0^2 + 2\beta i\omega)\, p^*(a,\omega) = -\left(\frac{d^2 P_a}{dt^2}\right)^*$$

If $\omega << \omega_0$, $p^*(a,\omega) = -\frac{1}{\omega_0^2}\left(\frac{d^2 P_a}{dt^2}\right)^*$ (41)

and if $\omega = \omega_0$,

$$p^*(a,\omega_0) = -\frac{1}{2i\beta\omega_0}\left(\frac{d^2 P_a}{dt^2}\right)^*_{\omega=\omega_0} \qquad (42)$$

<u>The Sound Produced by a Bubble in a Flow Past a Cylinder</u>

A knowledge of the position of a bubble as a function of time as the bubble moves past a cylinder obviously enables the determination of the external pressure experienced by bubble as a function of time. The acoustic response depends, however, not on this pressure directly but on its second time derivative, which may be found as follows:

$$P_a = P_a\left(x(t),\, y(t)\right)$$

$$\therefore \frac{dP_a}{dt} = \frac{\partial P_a}{\partial x}\frac{dx}{dt} + \frac{\partial P_a}{\partial y}\frac{dy}{dt}$$

and so $$\frac{d^2P_a}{dt^2} = \frac{\partial^2 P_a}{\partial x^2}\left(\frac{dx}{dt}\right)^2 + 2\frac{\partial P_a}{\partial x\partial y}\frac{dx}{dt}\frac{dy}{dt} + \frac{\partial^2 P_a}{\partial y^2}\left(\frac{dy}{dt}\right)^2 + \frac{\partial P_a}{\partial x}\frac{d^2x}{dt^2} + \frac{\partial P_a}{\partial y}\frac{d^2y}{dt^2}$$

Numerical integration of the equations of motion gives $x(t)$, $y(t)$, $\frac{dx}{dt}$ and $\frac{dy}{dt}$ and so at any instant $\frac{d^2P_a}{dt^2}$ may be calculated.

Figure 8 shows the results of plotting $\frac{d^2P_a}{dt^2}$ as a function of time. Both diagrams refer to a bubble with $P/a = 10^2$ and $f_e = 10^4$ but the upper diagram applies to a bubble initially at (-20, 0.5) and the lower to a bubble initially at (-20, 0.3). In each case the higher peaked curve shows a plot of $\frac{d^2P_a}{dt^2}$ for a bubble constrained to move along its original streamline. There is an arbitrary time origin (the same for all curves) but it may be approximately located by noting that the maximum of $\frac{d^2P_a}{dt^2}$ for a bubble on a streamline occurs when the bubble is on the line $x = 0$.

The most noticeable feature of these plots is the reduction in the height of the maxima for the bubbles whose

FIGURE 8 : $\frac{d^2 P_a}{dt^2}$ vs. t

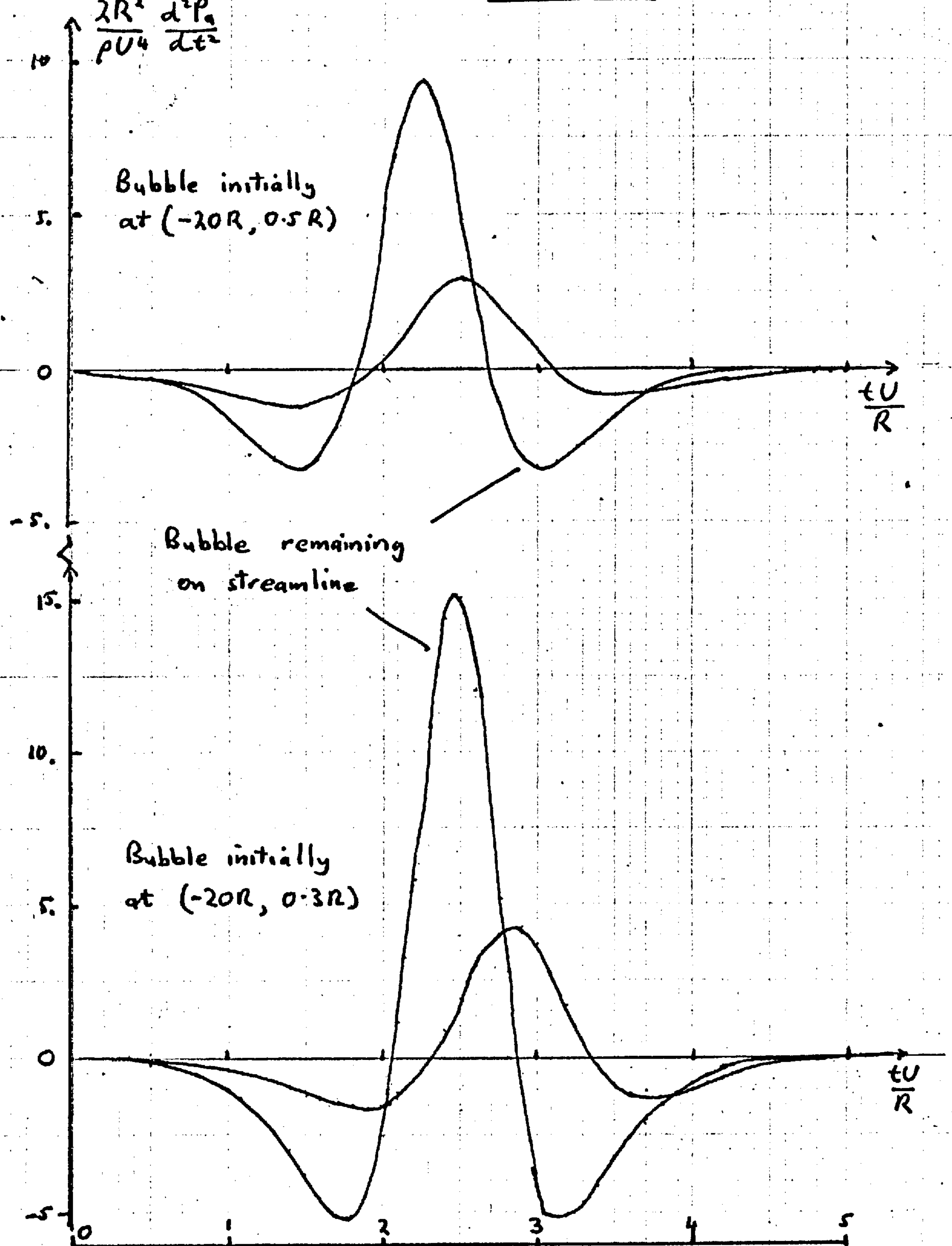

motion is determined by equation 32. Also the positive pulse is broadened and occurs at a later time. Because a bubble near the cylinder is deflected further from the cylinder than the corresponding fluid particle we would expect the bubble to be moving in a pressure field which changes more gradually spacewise: because the bubble has a basic acceleration ignoring the drag of three times that of the fluid it was at least possible that the bubble might traverse the pressure trough at right angles to the flow at a fast enough rate to more than compensate this slower space variation. Figure 8 shows that this does not in fact happen.

As a concomitant of the more gradual variation of $\frac{d^2P_a}{dt^2}$ with time we would expect the frequency spectrum of $\frac{d^2P_a}{dt^2}$ to fall off at a faster rate than that for a bubble constrained to move along a streamline. Figure 9 shows the Fourier transform of $\frac{d^2P_a}{dt^2}$ for a bubble originally at (-20, 0.5) and, on the same graph, the corresponding transforms for bubbles remaining on the streamlines through (-20, 0.5) and (-20, 0.05). The two curves corresponding to bubbles through the same point show very little difference although the expected lower values at higher frequencies are in evidence. All three

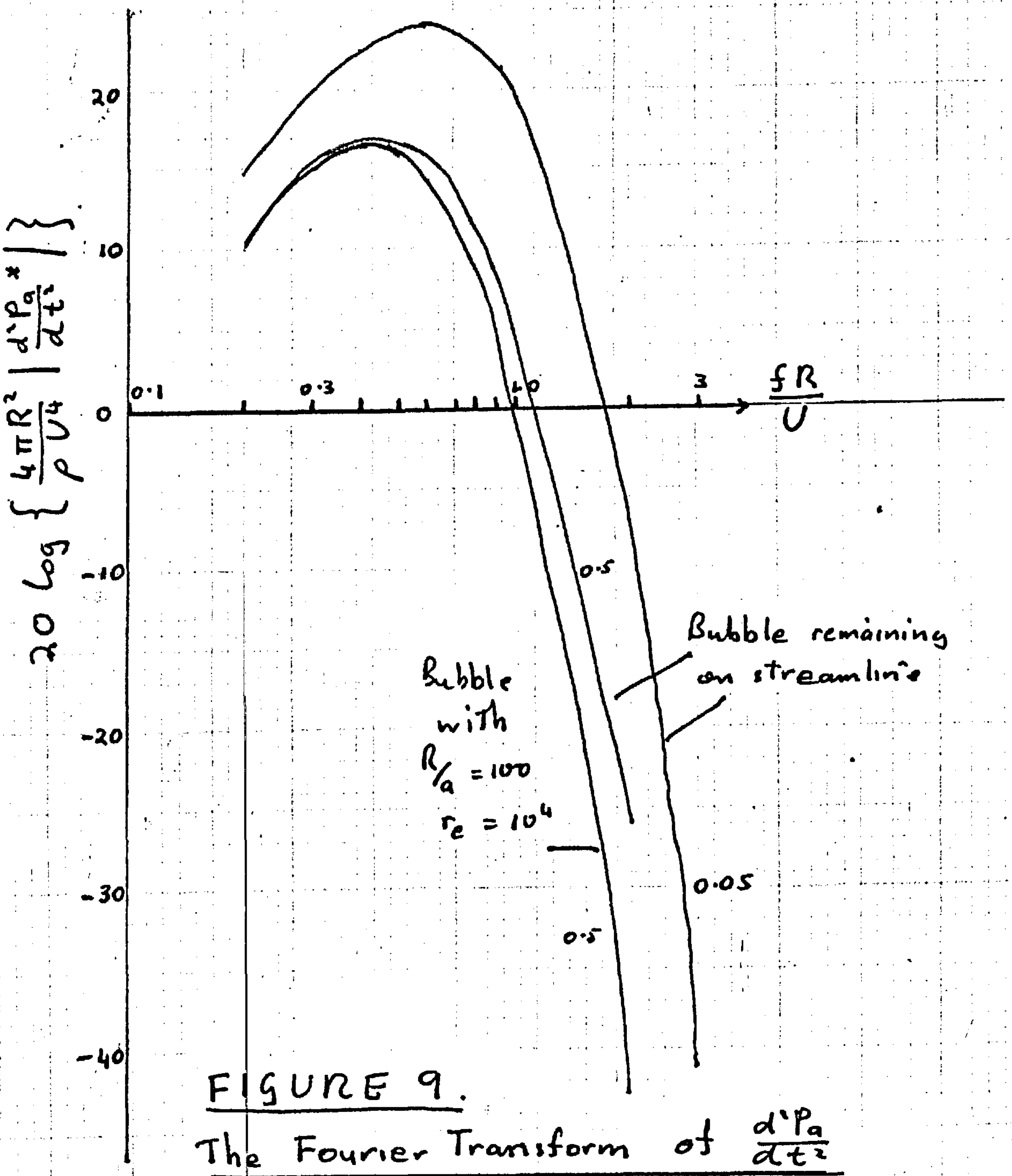

FIGURE 9.

The Fourier Transform of $\frac{d^2 P_a}{dt^2}$

(The numbers 0·5, 0·05 on plot indicate original distance of bubble from stagnation streamline) curves have a maximum at a frequency less than $\frac{U}{R}$ and fall off very rapidly for frequencies greater than $\frac{U}{R}$.

The modulus of the Fourier transform $p^*(a, \omega_o)$ will be much less than $p^*(a, \omega)$ if $\omega \ll \omega_o$

$$\frac{\omega_o}{2B} \left| \left(\frac{d^2 P_a}{dt^2} \right)^*_{\omega = \omega_o} \right| \ll \left| \left(\frac{d^2 P_a}{dt^2} \right)^*_{\omega} \right|$$

This is immediate from equations 41 and 42
That is, if

$$20 \operatorname{Log} \frac{\omega_o}{2B} + 20 \operatorname{Log} \left| \left(\frac{d^2 P_a}{dt^2} \right)^*_{\omega_o} \right| \ll 20 \operatorname{Log} \left| \left(\frac{d^2 P_a}{dt^2} \right)^*_{\omega} \right|$$

For a bubble with one atmosphere internal pressure $20 \operatorname{Log} \frac{\omega_o}{2B} \approx 37.5$. From Figure 9 we can now conclude that if ω_o is greater than about $2\,U/R$ the sound at the resonance frequency will be negligible compared to the sound from the frequencies near $0.4\,U/R$. In practice, ω_o is very much greater than U/R and as there is no reason why $\left| \left(\frac{d^2 P_a}{dt^2} \right)^* \right|$ should not continue its rapid decrease with increasing frequency we conclude that the sound produced near the resonance frequency is a negligible fraction of the total sound.

This being so, we may write the total acoustic bubble wall pressure to a high approximation as

$$p(a,t) = \frac{1}{\omega_o^2} \frac{d^2 P_a}{dt^2}.$$

The plot of $\frac{d^2 P_a}{dt^2}$ versus time is thus just the waveform of the radiated sound enlarged by the constant factor $-\omega_0^2$. Figure 10 is a plot of $\frac{d^2 P_a}{dt^2}$ for bubbles with $r_e = 10^4$, $R/a = 50$ which were originally at different distances from the fluid stagnation streamline. The actual distances are shown on the plots. It can be seen that certain curves end abruptly. The end points are within 0.05 dimensionless time units of impact with the cylinder.

The ordinates may be converted into absolute sound levels by multiplication by $\frac{1}{2}\rho \frac{U^4}{R^2} \frac{1}{\omega_0^2}$. If a = 0.1 cms, R = 5 cms, U = 5 metres/sec. then the level 10 of the ordinates corresponds to an acoustic wall pressure of 30 microbars.

Finally, if we revert to Figure 8 we see that the peak sound pressures obtained from the use of our equation of motion are less than those obtained by Strasberg's assumptions of streamline motion. We may conclude that bubbles which do not strike the cylinder can have a reduction in the peaks of up to about 5 db. For bubbles larger than $R/10$ we cannot make any deductions and the fact that our bubbles appear to strike the

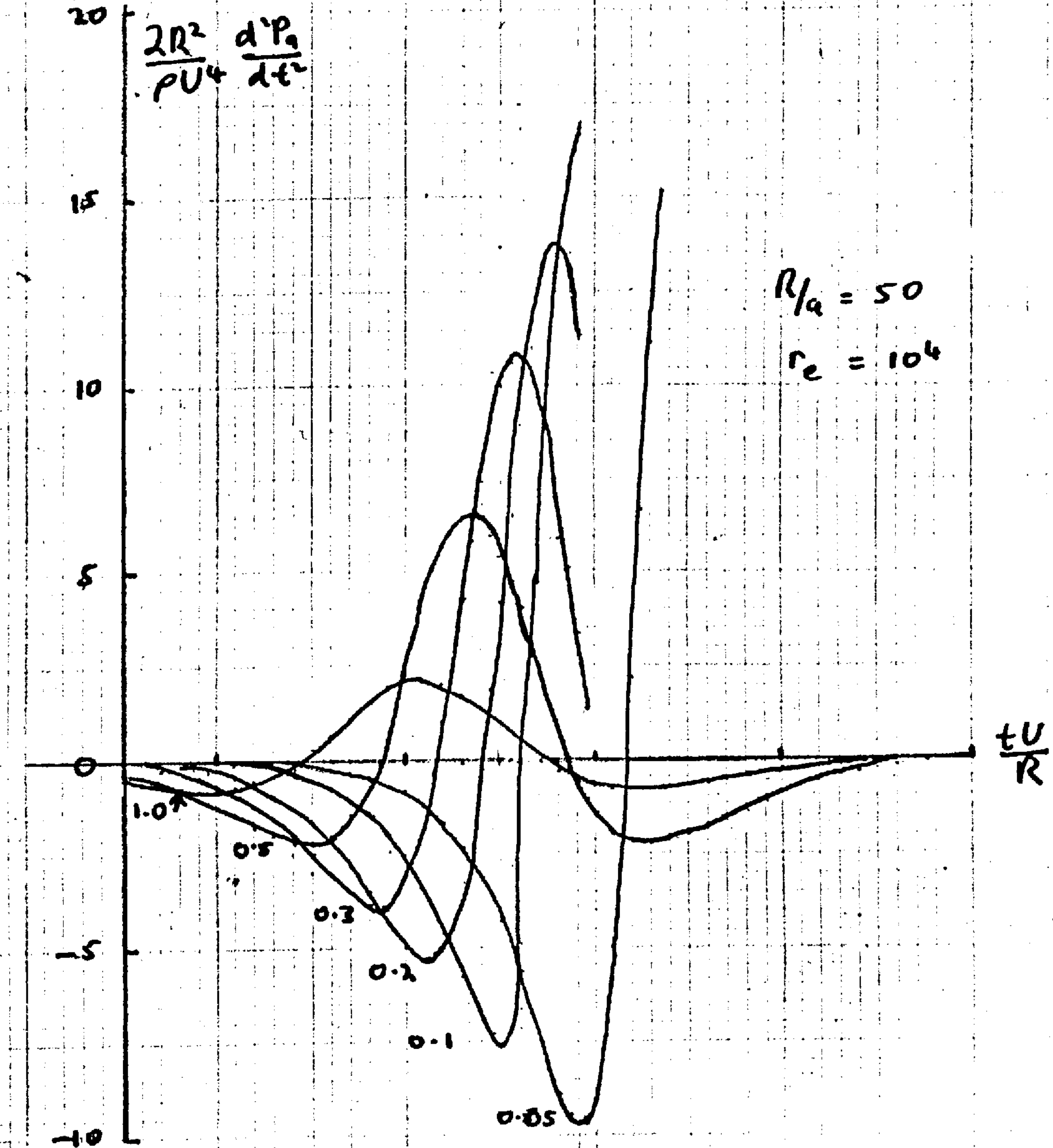

FIGURE 10 $\frac{d^2P_a}{dt^2}$ vs t for bubbles at various distances from stagnation streamline

cylinder if they are originally near the stagnation streamline raises doubts about the relevance of Strasberg's results obtained for a bubble actually moving on the cylinder surface.

Additional sources of sound from a Bubbly Flow Past an Obstacle

We have seen that for a wide range of the flow parameters bubbles originally near the stagnation streamline of a cylinder move towards the cylinder and, whether they actually strike the cylinder or not, are so fiercely decelerated that the larger bubbles are likely to disintegrate. The resulting bubble fragments would continue to move downstream around the cylinder and there meet incoming bubbles which were once originally further off the stagnation streamline. The rearward surface of the cylinder is thus likely to be the scene of both bubble disintegrations and coalescences, two processes which, as Strasberg first pointed out, provide a decaying sinusoidal pulse of sound each time they occur.

For example, suppose a bubble of radius a splits into two bubbles, the smaller ~~of which~~ having radius αa . At any instant a balance of the normal stresses across the wall of this bubble requires

$$P = P_a + p(\alpha a, t) + \frac{2\sigma}{\alpha a},$$

where the symbols have their previous meanings but where the variation of the ambient pressure with time is omitted so that

$$\frac{\partial^2 p}{\partial t^2}(\alpha a, t) + 2B\frac{\partial p}{\partial t}(\alpha a, t) + \omega_0^2 p(\alpha a, t) = 0$$

where $2B = \frac{3\gamma P}{\rho c a \alpha}$ and $\omega_0^2 = \frac{3\gamma P}{\alpha^2 a^2 \rho}$.

At the moment of formation, t = o , say, of the bubble the internal pressure within this bubble is just the internal pressure of the parent bubble. We then have

$$P_a + \frac{2\sigma}{a} = P_a + p(\alpha a, 0) + \frac{2\sigma}{\alpha a}$$

i.e., $p(\alpha a, 0) = \frac{2\sigma}{a}\left(1 - \frac{1}{\alpha}\right)$

Making the simplest possible assumption we set $\frac{\partial p}{\partial t}(\alpha a, 0)$ = to o and find that the acoustic wall pressure varies as

$$p(\alpha a, t) = \frac{2\sigma}{a}\left(1 - \frac{1}{\alpha}\right)e^{-Bt}\cos\omega_0 t$$

$$(\omega_0 >> B)$$

which has a maximum amplitude of $\frac{2\sigma}{a}\left(1 - \frac{1}{\alpha}\right)$. If a = 0.1 cms, σ = 80 dynes/cm and $\alpha = \frac{1}{10}$ this has the value 1.4 x 10^4 microbars, and so bubble disintegration must be regarded as a significant source of sound energy.

Sound which, moreover, is at the resonant frequency of the daughter bubbles.

The sound from a bubble coalescence is treated in a similar manner, and again more sound is produced if there is a large disparity in the sizes of the bubbles involved.

A second possible source of sound which will now be investigated is the excitation of the bubbles by the fluctuating pressures which occur in the wake of the obstacle. A typical frequency in the turbulence behind a cylinder is of order U/R which is always very much less than the resonance frequency of the bubbles for flows and bubble sizes of practical importance. The acoustic pressure at the bubble wall is then given by

$$p(a,t) = -\frac{1}{\omega_0^2}\frac{d^2 P_a}{dt^2}.$$

The turbulence pressure fluctuations have amplitude of order $\rho U^2 \alpha^2$ where α is now the turbulence intensity. Taking α = 0.1, R = 10 cm, U = 5 metres/sec and a = 0.1 cms, then

$$p(a,t) \doteq \frac{1}{\omega_0^2}\frac{U^2}{R^2}\alpha^2 \rho U^2 = 0.01 \text{ microbars}$$

- a decidedly low level of sound.

However, there is a completely different situation if we look at the wake behind a bubble caused by the relative motion of the bubble and the liquid. Near the cylinder a bubble which is assumed to obey our basic equation of motion (equation 32) has a slip velocity relative to the liquid of the same order as the stream velocity, U. A typical frequency in the wake behind a bubble can therefore be as high as $\frac{U}{a}$ which can be comparable, greater even, than the resonance frequency of the bubble. The two will be comparable if U is of order $\left(\frac{3\gamma P}{\rho}\right)^{\frac{1}{2}}$, or 20 meters/ 1 sec if P is one atmosphere, and when this happens we can expect significant amounts of sound at the resonance frequency.

It is not necessary, however, that the slip velocity be of order U before the flow about a bubble has frequencies in it comparable to ω_0. Levich[21] has pointed out that a bubble moving at high Reynold's number R_e (defined as before) has a stress boundary layer of thickness $a R_e^{-\frac{1}{2}}$, within which the fluid velocity is of the same order as the slip velocity. Any instability within this layer will accordingly have a characteristic frequency $\frac{|\underline{w}-\underline{u}|}{a} R_e^{\frac{1}{2}}$. This is possibly the explanation of the sound produced by bubbles of radii greater than about 0.1 cms ascending under gravity, with smaller bubbles giving scarcely measurable sound levels. Not only do the larger bubbles have a higher velocity but, because the Reynold's numbers are larger there is a greater likelihood of instability within the wakes and boundary layers.

Strasberg attributes the sound from rising bubbles to the erratic paths followed by the larger bubbles. It has not been definitely confirmed, however, that such bubbles do, in fact, move in paths which have abrupt changes of direction. Dr D. Moore of Imperial College has told the author that his observations would suggest that the bubbles in fact move along regular spirals. Certainly, if irregularity is confirmed, the mechanism which causes it is unknown.

If we refer back to Figure 5, we can demonstrate that if the fluid contained a constant density of bubbles upstream of the cylinder there will not be a constant density of the bubbles downstream of the cylinder. For consider the bubble path furthest from the stagnation streamline. Downstream of the cylinder this path is diverging from the original streamline and will ultimately lie along another streamline when the bubble velocity will be tending towards the constant velocity U. This is because, far from the cylinder, the force due to the pressure field around the cylinder becomes much less than the viscous drag force which will always be constraining the bubble to move with the fluid. None of the bubble paths shown in Figure 5 intersect: were they to do so then, necessarily, the bubble density would not remain constant. If no paths at all intersect, then because the bubbles at large distances upstream and downstream of the cylinder are moving with essentially the stream velocity and because the bubble path discussed before does not return to its original streamline, conservation of total bubble volume necessarily requires that the bubble density far downstream of the cylinder is less than that upstream.

Now the velocity of sound in a liquid decreases with increasing bubble density, so we may conclude that far downstream the cylinder's wake will have a higher speed of sound than the adjacent fluid. Consequently, a polar plot of the sound intensity produced by a bubbly flow will have a minimum in the direction corresponding to the wake - the sound waves travelling initially in the downstream direction will be refracted outwards.

Appendix A

A listing of the programme which produced Figure 4 is given in this appendix.

In the programme, BUBRAD and CYLRAD are the locations of the bubble and cylinder radii respectively. The velocity of the fluid far from the cylinder is stored at VEL and its kinematic viscosity at ANV. The initial y coordinates of the bubble are stored in the array YIN.

x x x x x

References

1. Lighthill, M.J., 1952. On Sound Generated Aerodynamically. I. General Theory. Proc. Roy. Soc. A, 211, 564-587.

2. Lighthill, M.J., 1954. On Sound Generated Aerodynamically. II. Turbulence as a source of sound. Proc. Roy. Soc. A, 222, 1-32.

3. Curle, N., 1955. The Influence of Solid Boundaries upon Aerodynamic Sound. Proc. Roy. Soc. A, 231, 505-514.

4. Phillips, O.M., 1956. On the Aerodynamic Surface Sound from a Plane Turbulent Boundary Layer. Proc. Roy. Soc. A, 234, 327-335.

5. Lighthill, M.J., 1961. The Bakerian Lecture. Sound Generated Aerodynamically. Proc. Roy. Soc. A, 267, 147-182.

6. Powell, A., 1960. Aerodynamic Noise and the Plane Boundary. J. Acoust. Soc. Amer. 32, 8, 982.

7. Doak, P.E., 1959. Acoustic Radiation from a Turbulent Fluid containing Foreign Bodies. Proc. Roy. Soc. A, 254, 129-145.

8. Ffowcs Williams, J.E., 1964. Sound Radiation from Turbulent Boundary Layers formed on Compliant Surfaces. J. Fluid Mech. 22, 347-358.

9. Ffowcs Williams, J.E., 1966. The Influence of Simple Supports on the Radiation from Turbulent Flow near a Plane Compliant Surface. J. Fluid Mech. 26, Part 4, 641-649.

10. Leppington, F.G., 1966. Unpublished.

11.)
12.) Macdonald, H. M., 1915. A class of Diffraction Problems. Proc. Lond. Math. Soc.

13. Pearcey, 1956. Table of the Fresnel Integral. Cambridge 1956.

14. Peebles and Garbor, 1953. Chem. Engr. Progress.

15. Landweber and Yih, 1956. Forces, Moments and Added Masses for certain Rankine Bodies. J. Fluid Mech, 1.

16. Zahm, A.F., 1927. Flow and Drag Formulae for Simple Quadries. N.A.C.A. Report No. 253.

17. Milne Thompson. Theoretical Hydrodynamics (Macmillan).

18. Minnaert, M. Phil. Mag. 16, 235 (1933).

19. Strasberg, M. Gas Bubbles as Sources of Sound in Liquids. J.A.S.A. 28, 20 (1956).

20. Zahm. N.A.C.A. Report No. 253, 1926.

21. Levich. Physico-Chemical Hydrodynamics.

```
C          PROGRAM TO SHOW BUBBLE PATHS FOR DIFFERENT INITIAL
                                                    POSITIONS
C
      DIMENSION SX(161),SY(161),XSP(161),YSP(161),YIN(6)
      COMMON LH1,LH2,LH3,LH4,LH5,BUBRAD,CYLRAD,HOLD,I
     1 ,AK,X,Y,VX,VY
      VXDIF(VX,X,Y)=VX-(1.-(X*X-Y*Y)/(X*X+Y*Y)**2)
      VYDIF(VY,X,Y)=VY-(-2.*X*Y/(X*X+Y*Y)**2)
      VSLIP(VX,VY,X,Y)=SQRT(VXDIF(VX,X,Y)**2+VYDIF(VY,X,Y)**2)
      ACX(VX,VY,X,Y)=FAC*2.*X*(X*X-3.*Y*Y-1.)/(X*X+Y*Y)**3
     1  -DRAG(VSLIP(VX,VY,X,Y),VXDIF(VX,X,Y),C,COB,RE)
      ACY(VX,VY,X,Y)=FAC*2.*Y*(3.*X*X-Y*Y-1.)/(X*X+Y*Y)**3
     1  -DRAG(VSLIP(VX,VY,X,Y),VYDIF(VY,X,Y),C,COB,RE)
      CALL START
      READ (5,1003) YIN
 1003 FORMAT (6F4.2)
      FAC=3.
      BUBRAD=0.1
      CYLRAD=10.0
      VEL=500.
      ANU=0.01
      COB=CYLRAD/BUBRAD
      RMIN2=(1.+BUBRAD/CYLRAD)**2
      RE=2.*VEL*BUBRAD/ANU
      ER=1./RE
      DO 100 JJ=1,2
      DO 101 J=1,6
      Y=YIN(J)
      IF (JJ.EQ.2)  FAC=1.
      AK=1.
      LH1=0
      LH2=0
      LH3=0
      LH4=0
      LH5=0
      X=-20.
      I=0
      T=0.
      IA=0
      VX=1.-(X*X-Y*Y)/(X*X+Y*Y)**2
      VY=-2.*X*Y/(X*X+Y*Y)**2
    8 CONTINUE
      IF (I.EQ.0) GO TO 204
      HT=BUBRAD/CYLRAD/3.6/VSLIP(VX,VY,X,Y)
      CALL HFIND(HT,H,HOLD)
      GO TO 205
  204 CONTINUE
      H=1.0E-06
  205 CONTINUE
```

```
       IF (LH5.EQ.1) GO TO 101
      IF (VSLIP(VX,VY,X,Y)-ER) 1,2,2
    1 C=1.
      GO TO 3
    2 C=2.
    3 IF (VSLIP(VX,VY,X,Y).EQ.0.) C=3.
      IF (JJ.EQ.2) C=3.
       IF (VX.LT.0.0.AND.X.LE.-5.0) GO TO 101
      X1=X
      Y1=Y
      VX1=VX
      VY1=VY
      X2=X+0.5*H*VX
      Y2=Y+0.5*H*VY
      VX2=VX+0.5*H*ACX(VX1,VY1,X1,Y1)
      VY2=VY+0.5*H*ACY(VX1,VY1,X1,Y1)
      X3=X+0.5*H*VX2
      Y3=Y+0.5*H*VY2
      VX3=VX+0.5*H*ACX(VX2,VY2,X2,Y2)
      VY3=VY+0.5*H*ACY(VX2,VY2,X2,Y2)
      X4=X+H*VX3
      Y4=Y+H*VY3
      VX4=VX+H*ACX(VX3,VY3,X3,Y3)
      VY4=VY+H*ACY(VX3,VY3,X3,Y3)
      X=X+H*(VX+2.*VX2+2.*VX3+VX4)/6.
      Y=Y+H*(VY+2.*VY2+2.*VY3+VY4)/6.
      VX=VX+H*(ACX(VX1,VY1,X1,Y1)+2.*ACX(VX2,VY2,X2,Y2)
     1   +2.*ACX(VX3,VY3,X3,Y3)+ACX(VX4,VY4,X4,Y4))/6.
      VY=VY+H*(ACY(VX1,VY1,X1,Y1)+2.*ACY(VX2,VY2,X2,Y2)
     1   +2.*ACY(VX3,VY3,X3,Y3)+ACY(VX4,VY4,X4,Y4))/6.
      IF(X.GT.4.) GO TO 101
      I=I+1
      IF(X.LT.-5.) GO TO 8
      IF (X*X+Y*Y-RMIN2) 210,210,211
  210 CONTINUE
      XX=4.-Y1
      YY=15.-X1
  200  WRITE (6,201) X,Y,T,H
  201 FORMAT (1H ,3F20.3,E10.2)
      CALL PLOT (XX,YY,2)
      XX=XX+0.1
  105 CALL PLOT(XX,YY,2)
      GO TO 101
  211 CONTINUE
      T=T+H
      IT=T*1.0E05+0.3
      T=IT
      T=T/1.0E05
      IF (ABS(T-0.05*AK).GE.1.0E-05) GO TO 8
      K=AK
      AK=AK+1.
      XX=4.-Y
      YY=15.-X
      IF (XX.LT.0.) GO TO 90
      IF (ABS(Y).GT.5.) GO TO 93
       IF (K.EQ.1) GO TO 212
```

```
      IF (JJ.EQ.2.AND.MOD(K,2).EQ.0) GO TO 212
   48 CALL PLOT (XX,YY,2)
      GO TO 8
  212 CALL PLOT (XX,YY,3)
      GO TO 8
   90 WRITE(6,92) J
   92 FORMAT(1H 25HBUBBLE MOVING UPSTREAM J=,I1)
      GO TO 101
   93 WRITE(6,94) J
   94 FORMAT(1H ,44HBUBBLECROSSSTREAN DISPLACEMENT EXCESSIVE
                                                J=, I1)
       GO TO 101
  101 CONTINUE
  100  CONTINUE
      CALL SPHERE   (J)
      STOP
      END

      FUNCTION DRAG(A,B,C,COB,RE)
      IF (C-2.) 4,5,6
    4 DRAG=COB*(18./RE+3.375*A)*B
      RETURN
    5 DRAG=0.75*COB*(28./RE**0.85*A**0.15+0.48*A)*B
      RETURN
    6 DRAG=0.
      RETURN
      END
```

```
      SUBROUTINE HFIND(HT,H,HOLD)
      COMMON LH1,LH2,LH3,LH4,LH5,BUBRAD,CYLRAD,HOLD,I
     1 ,AK,X,Y,VX,VY
      IF (HT.GE.0.05) GO TO 21
      IF (HT.LT.0.05.AND.HT.GE.0.01) GO TO 22
      IF (HT.LT.0.01.AND.HT.GE.0.001) GO TO 23
      IF (HT.LT.0.001.AND.HT.GE.0.0001) GO TO 24
      IF (HT.LT.0.0001.AND.HT.GE.0.00001) GO TO 25
      IF (HT.LT.0.00001) GO TO 26
   21 H=0.05
      IF (H.GT.HOLD.AND.LH1.NE.0) GO TO 22
      IF (H.GT.HOLD.AND.LH2.NE.0) GO TO 23
      IF (H.GT.HOLD.AND.LH3.NE.0) GO TO 24
      IF (H.GT.HOLD.AND.LH4.NE.0) GO TO 25
      GO TO 20
   22 H=0.01
      IF (H.GT.HOLD.AND.LH2.NE.0) GO TO 23
      IF (H.GT.HOLD.AND.LH3.NE.0) GO TO 24
      IF (H.GT.HOLD.AND.LH4.NE.0) GO TO 25
      LH1=LH1+1
      GO TO 76
   23 H=0.001
      IF (H.GT.HOLD.AND.LH3.NE.0) GO TO 24
      IF (H.GT.HOLD.AND.LH4.NE.0) GO TO 25
      LH2=LH2+1
      GO TO 75
   24 H=0.0001
      IF (H.GT.HOLD.AND.LH4.NE.0) GO TO 25
      LH3=LH3+1
      GO TO 74
   25 H=0.00001
      LH4=LH4+1
      IF (LH4-10) 20,70,20
   70 LH4=0
      LH3=LH3+1
   74 IF (LH3-10 ) 20,71,20
   71 LH3=0
      LH2=LH2+1
   75 IF (LH2-10) 20,72,20
   72 LH2=0
      LH1=LH1+1
   76 IF (LH1-10) 20,73,20
   73 LH1=0
      GO TO 20
   26 WRITE (6,27) HOLD,X,Y
   27 FORMAT (1H ,27 HINCREASE IN H TOO SMALL H =,E10.2,2F10.4)
      LH5=1
      RETURN
```

```
   20  HOLD=H
        RETURN
       END
```

```
       SUBROUTINE SPHERE (J)
       DIMENSION SX(161),SY(161),XSP(161),YSP(161),YIN(24)
       IF (J.EQ.1) RETURN
       CALL PLOT (3.,15.,3)
       I=1
   32  XSP(I)=-1.+FLOAT(I-1)*0.025
       YSP(I)=SQRT(1.-XSP(I)**2)
       I=I+1
       IF (I-81) 32,32,33
   33  XSP(I)=1.-FLOAT(I-81)*0.025
       YSP(I)=-YSP(I-80)
       I=I+1
       IF (I-162) 33,34,34
   34  DO 17 I=1,161
       SX(I)=4.+XSP(I)
       SY(I)=15.+YSP(I)
       CALL PLOT (SX(I),SY(I),2)
   17  CONTINUE
       RETURN
       END
```